Engineering Research Journal

journal homepage: https://erj.journals.ekb.eg/

Pounding interaction among adjacent MRF multi-story buildings and associated performance levels under strong ground motion

Abbas Moustafa [1], Magdy Genidy[2], Hesham Tahon[3,] *, Hany Ragab[4]

[1] Professor, Civil Engineering Department, Faculty of Engineering, Minia University
[2] Associate Professor of R.C. Structures, Faculty of Engineering, Mataria, Helwan University
[3]Ph.D. Student, Civil Engineering Department, Faculty of Engineering, Mataria, Helwan University
[4]Assistant Professor, Construction Department, Faculty of engineering, Egyptian Russian University

*Corresponding author E-mail: hishamd01248@m-eng.helwan.edu.eg@gmail.com

Abstract. The main objective of this paper is to assess the performance of neighboring colliding buildings in series with insufficient separation distances. The study focuses on the simultaneous pounding of three structures with various heights located side by side to each other. A numerical simulation of three adjacent buildings of 3-story, 6-story, and 12-story MRF buildings are combined to produce an alignment configuration. This configuration of adjacent buildings is subjected to strong ground motion of El Centro (1940) and Kobe (19) as input excitation. The structural model for three buildings considers plastic hinges at every beam-column connection at both ends, which generates enough plastic hinges and gives a more realistic approach. The nonlinear direct integration time-history analysis is performed for the evaluation of the response demands of the alignment configuration of the adjacent buildings using structural analysis ETABS Ultimate C software. The structural response parameters are relative displacement, induced pounding force, story drift, story shear, story acceleration, input/dissipated energy, hysteretic behavior, and tracing the changing of plastic hinges' status. The response parameters under the pounding effect are compared to the corresponding response parameters of the no-pounding case from one side and the different gap distances case from the other side. Based on the results obtained, it has been concluded that the severity of the seismic pounding effects depends on the dynamic properties of each building, the dynamic characteristics of input excitation, separation gap sizes, building height ratio, and the alignment position of the building in series: whether interior building with potential two-sided impacts or an exterior building with potential one-sided pounding. The numerical results prove the crucial role of pounding interaction among the three colliding buildings. The high-rise building (12-story) induces greater shear force and acceleration response demand at the contact case along the story level compared to the no-pounding case, while the response demands could be reduced in the shorter buildings. Finally, it has been concluded that the performance level of high-rise building (12-story) is significantly magnified, while the performance level of low-rise buildings (6-story and 3-story) is reduced.

Keyword: Adjacent Buildings series, ETABS software, Gap distance, Inelastic structure, Nonlinear dynamic time history analysis, Performance level, Plastic hinges, Seismic pounding.

DOI: 10.21608/erj.2025.375005.1226
Received 12 April 2025; Received in revised form 02 June 2025; Accepted 11 June 2025
Available online 01 September 2025

1. Introduction

During earthquakes, the repeated pounding of neighboring buildings in sequences causes damage that can vary from minor non-structural local damage to significant structural global damage that could result in a building's complete failure, Fig.1.

1. Literature review

Numerous investigations in the literature have been involved with the effect of seismic pounding on the response of adjacent buildings. Furthermore, a number of researches investigated how the dynamic characteristics of buildings such as (their mass, number of stories, and overall height) influence the response of adjacent buildings subjected to seismic pounding (in terms of story acceleration, story displacement, inter-story drift, impact force, etc.). Those investigations can be classified into three main categories or aspects. Researches on buildings with fixed bases is included in the first one; research on structures with base isolation systems is included in the second; and research that consider soil-structure interaction is included in the third aspect.

The 1985 Mexico Earthquake (Anagnostopoulos 1988) | The 1985 Mexico earthquake (Johnmartin 2018, NCEI 2018) | The 2011 Van earthquake (Ozmen et al. 2013, Aykutozdemir 2018)

Fig. 1. Damage in neighboring structures of various height due to pounding phenomena

1.1.1 Buildings with Fixed Bases exposed to pounding

Elwardany et al. [1] conducted an analysis to evaluate the seismic pounding among adjacent buildings with different fundamental periods. They concluded that the arrangement of adjacent buildings significantly affected the pounding-induced response. For example, the presence of flexible buildings at the cluster's edge caused magnification in the pounding forces. Similarly, Efraimiadou et al. [2] numerically studied the pounding-induced response of a row of buildings with different arrangements and parameters. They compared pounding and no-pounding cases in terms of maximum and residual inter-story drift, as well as maximum story acceleration. Naturally, it was discovered that pounding significantly increases the buildings' response. However, in some structures when the inter-story drift was dropped, it was found beneficial. The last conclusion is consistent with the findings in [3]. Based on their numerical study, Sołtysik and Jankowski [4] concluded that pounding may be crucial in reducing the response of the first adjacent building, even though it increases the story displacement and story acceleration of the second one. To evaluate the influential parameters on seismic pounding, Crozet et al. [5, 6] conducted a sensitivity analysis on adjacent buildings based on Monte Carlo simulations. It was observed that the most significant factor influencing the impact force was the ratio of the frequencies of adjacent structures. Although most numerical studies have ignored masonry infill, Elwardany et al. [7, 8] demonstrated that considering masonry infill can minimize the pounding effect relative to bare frame. This was correlated to the fact that seismic pounding comprises higher-level vibration mode shapes. At the same time, these mode shapes were distinguished by significant deformation of the stories. As a result of their increased rigidity, infilled panels were certainly subjected to less deformations than bare panels. This contrasts with most simple structures, in which just the first vibration mode shape is dominant in no-pounding scenarios. In their analytical investigation, Ismail et al. [9] discovered similar results. They even proposed that the contribution of masonry infills to the

decrease of seismic pounding may be utilized by selecting a narrower seismic gap. Manoukas and Karayannis [10] conducted a comprehensive numerical investigation of the seismic interaction between reinforced concrete buildings, with a particular emphasis on structures with open first stories (pilotis) and the effect of asymmetric pounding. They proved that pilotis layouts substantially boosted the overall structural response, especially floor rotations, which might increase by up to nearly tenfold. Additionally, asymmetric pounding, both floor-to-floor and floor-to-column, amplified torsional vibrations and caused shear failures in columns, often exceeding allowable strength by substantial margins. Their findings emphasized the vital relevance of including these parameters in earthquake design and retrofitting procedures.

1.1.2 Buildings with Base isolation exposed to pounding

Previous research has proposed a number of resistant ways to protect structures from earthquake ground excitations. One of these ways involves installing a base isolation system among the superstructure and the foundations. Mavronicol et al. [11] focused their numerical analysis on pounding between a building separated with laminated rubber bearings and moat walls. The ground motion's orientation angle was discovered to have a significant effect on the building's pounding-induced response. As a result, it is important to carefully choose a suitable spacing size. Recently, Mavronicola et al. [12] verified similar findings for buildings with lead rubber bearings. Mahmoud and Janowski [13] analytically investigated the pounding-induced response of isolated and fixed-base structures. The isolated structures were equipped with high-damping rubber bearings. They demonstrated that if an isolated structure collided with another isolated or fixed-base structures, the isolated building's story response would remain almost constant throughout its height. Furthermore, the fixed-base building's story response fluctuated along its height. Pant and Wijeyewickrema [14] evaluated the performance of an isolated structure, a fixed-base structure, and a moat wall subjected to floor-to-column pounding. The lead rubber bearing was the chosen base isolation system. It was discovered that the columns of the structures failed due to flexure rather than shear, despite the fact that the floor-to-column pounding increased the shear requirements. Liu et al. [15] used numerical analysis to compare the pounding of structures using lead rubber bearing isolators and friction pendulum isolators. They found that friction pendulum isolators amplified the building's pounding-induced response more than lead rubber bearing isolators.

1.1.3 Buildings with soil-structure interaction considered

Although all the studies addressed previously ignored the effect of soil, some studies investigated the effect of soil-structure interaction on seismic pounding. The reason for this is because disregarding soil-structure interaction only applies to rock soils. Other types of soils, especially soft soils, have a significant influence on the pounding-induced response of buildings [16]. Buildings are constructed on several soil layers with varying characteristics. As a result, they clearly affect the properties of ground motion as it passes through the soil layers and reaches the ground surface [17]. This, in turn, affects the seismic response of buildings. As a result, the interaction between the building and the soil beneath it must be considered [18]. Fatahi et al. [19] conducted quantitative tests on the seismic pounding of surrounding pile-supported buildings. As a result, the soil-pile-structure interaction was taken into consideration. They advised that the combined effect of seismic pounding and soil-pile-structure interaction be considered in practice when designing neighboring buildings, as it had a significant impact on the results. Miarai and Jankowski [20] used shaking table experimental tests on two adjacent steel buildings with varying separation distances under the influence of various earthquakes that were scaled so that their response spectra matched the response spectra found in [21] for different soil types (hard rock, rock, etc.) in order to investigate the impact of soil type on the response of buildings subjected to seismic pounding. It was shown that the type of soil had a major impact on the response of adjacent buildings. However, the outcomes for various soil types differed based on the ground motion and pounding scenario. Therefore, it was determined that no particular type of soil increases the

buildings' reaction to seismic pounding. Naturally, soil-structure interaction was taken into consideration. It was clear that the impact forces increased with the increment of seismic duration. Furthermore, it was discovered that models exposed to longer excitations needed a larger seismic gap.

1.2 Analysis of previous literature review

Many previous researchers focused on studying the mutual pounding between only two adjacent structures while very few researches were concerned with the pounding of a series of structures. The ability to numerically and analytically evaluate adjacent buildings designs under seismic pounding has been significantly improved by the thorough examination of numerous analytical models in earlier discussions. As a result, theoretical research made it necessary to choose the geometric modeling strategy used for nearby structures. These structures can be shown as lamped masses, 2-D (planar frame) models, 3-D models, or single or multiple degrees of freedom buildings. Furthermore, techniques like reliability and fragility analysis, incremental dynamic analysis, and time-history analysis can be used to examine the pounding-induced response of such buildings.

1.3 Research methodology

The current research focuses on the effects of the seismic pounding among three buildings in series modelled as MDOF with different heights on the seismic response demands. A nonlinear 3D-FE modelling is developed to simulate the colliding between adjacent buildings side by side alignment. Different building models in height namely 12-story ,6-story, and 3-story moment resistance frame structures are attached together by using nonlinear gap element to produce the numerical model configuration. This configuration is subjected to strong earthquake excitations of El Centro (1940) and Kobe (19). For various gap distances in addition to buildings in-contact case, the impact of pounding is examined and thereafter compared with non-pounding model case. Nonlinear direct integration time-history analysis is carried out using the ETABS Ultimate C V20.3.0 Build 2929 [23]. Various responses quantities are assessed as relative displacements, induced impact force, acceleration time histories, story acceleration, story shear force, input/dissipated energy, hysteretic behavior, and trace the changing the status of plastic hinges formation by comparing the pounding case with no-pounding case from one side and comparing the different gap distances case from the other side. The global performance level of adjacent buildings has been evaluated by demand-capacity ratios for each building and comparing the in-contact case with case of fully separated buildings, while the local performance level has been evaluated by the status of every plastic hinge generated around the beam column connection.

2. Building performance level and damage state.

Conventional design codes do not explicitly establish a performance level. Modern performance-based seismic design entails setting performance levels and checking acceptance criteria for which a building is to be designed. By contrasting the computed values of the demand parameters—or, more simply, the "demands"—with the acceptance criteria, or "capabilities," for the intended performance level, the performance is evaluated. Frequently, "demand-capacity" ratios are used to compare the estimated demands and acceptance criteria. The terms "deformation-controlled" (ductile members that can resist inelastic deformations) and "force-controlled" (non-ductile members whose capacities are determined by strength) were typically distinguished in acceptance criteria for structural members.
The required level of performance for seismic resistant design can determine how much inelastic behavior is permitted in a structure. FEMA 356 [24] and ASCE 41-17 [25] criteria used the three frequently employed performance levels of Immediate Occupancy (IO), Life Safety (LS), and Collapse Prevention (CP) as a description of damage states regarding performance levels (Fig.2). According to

FEMA 356, allowable inter-story drift values of 1.0%, 2.0% and 5.0% for performance levels IO, LS, and CP were chosen for RC structures and for reinforcement rebar.

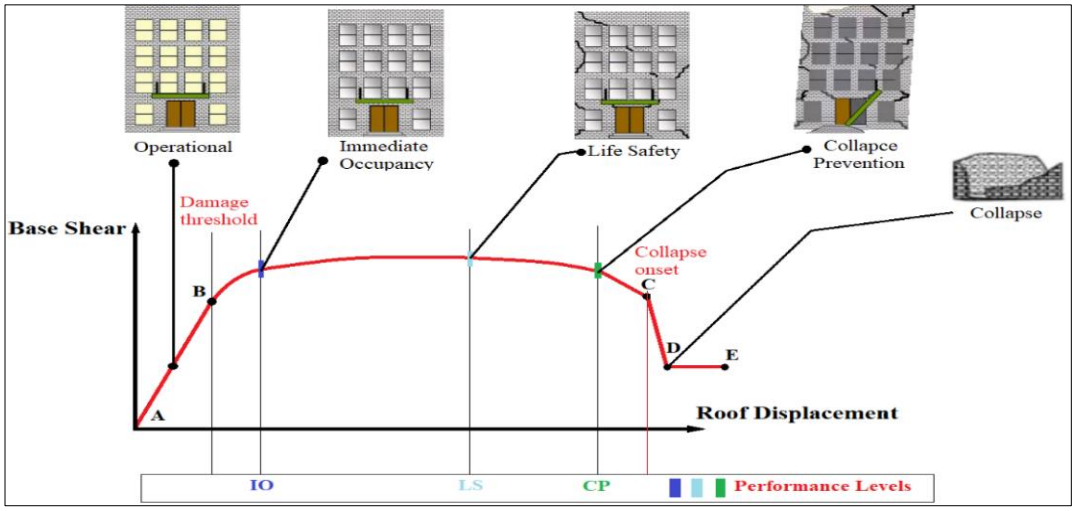

Fig. 2. Building performance level and corresponding damage state

Point B corresponds to the formation of the first plastic hinge (represents yielding) and point C corresponds to the ultimate capacity and marks the beginning of the degradation phase of the section and the drop of its strength. Residual stresses allow the section to resist to gravity loads (point D) until the ultimate deformation (point E) corresponding to the failure of the element. The points A, B, C and D calling modelling parameters.

3. Building and pounding models' assumptions

At the current research, the numerical model is consists of three aligned adjacent R.C-MRF with three, six and twelve-stories positioned at a separation distance named "d". There are two equally separation gap distances between the (12-story) building & (6-story) building from right side and between (12-story) building & (3-story) building from left side. The generated pounding forces impacting on the colliding buildings are estimated using a nonlinear gap element to numerically simulate the pounding.

3.1 Nonlinear Buildings models 'assumptions

The most effective method for assessing structures response to seismic excitations provided by ground acceleration records is time-history analysis method, which is a nonlinear dynamic analysis. The most powerful method for nonlinear analysis, Newmark time integration, is used to solve the governing equations of motion in a step-by-step nonlinear direct integration procedure. Dynamic earthquake loads gradually alter the structure with time intervals ($\Delta t = 0.02$ s). Series of short time increment are used to evaluate the structural response. For MDOF, the general equation of motion in incremental form is [26]:

$$\boldsymbol{M}\Delta\ddot{U}(t) + \boldsymbol{C}(t)\Delta\dot{U}(t) + \boldsymbol{K}(t)\Delta U(t) + F_p(t) = -\boldsymbol{M}\{\mathbf{1}\}\ddot{u}_g(t) \quad (1)$$

Where $\boldsymbol{M}$ is mass matrix, $\boldsymbol{C}$ is damping matrix and $\boldsymbol{K}$ is stiffness matrix. The vectors U is displacement vector and dot indicate differentiation with respect to time. $\ddot{u}_g$ is the earthquake acceleration's single component. $\{1\}$ is a vector of ones. F_p is the force vector due to impact (pounding force) More sensible insight to the equation is presented by the equation no.2.

The coefficients multiplying the mass and stiffness matrices are calculated based on carefully selected frequencies of the studied buildings.

$$\begin{bmatrix} m_{xn} & 0 & 0 \\ 0 & m_{ym} & 0 \\ 0 & 0 & m_{zl} \end{bmatrix} \begin{Bmatrix} \ddot{u}_{xn} \\ \ddot{u}_{ym} \\ \ddot{u}_{zl} \end{Bmatrix} + \begin{bmatrix} c_{xn} & 0 & 0 \\ 0 & c_{ym} & 0 \\ 0 & 0 & c_{zl} \end{bmatrix} \begin{Bmatrix} \dot{u}_{xn} \\ \dot{u}_{ym} \\ \dot{u}_{zl} \end{Bmatrix} + \begin{bmatrix} k_{xn} & 0 & 0 \\ 0 & k_{ym} & 0 \\ 0 & 0 & k_{zl} \end{bmatrix} \begin{Bmatrix} u_{xn} \\ u_{ym} \\ u_{zl} \end{Bmatrix} + \begin{Bmatrix} \overline{F}_{P1} \\ -\overline{F}_{P1} \\ \overline{F}_{P2} \\ -\overline{F}_{P2} \end{Bmatrix} = - \begin{bmatrix} m_{xn} & 0 & 0 \\ 0 & m_{ym} & 0 \\ 0 & 0 & m_{zl} \end{bmatrix} \begin{Bmatrix} 1 \\ 1 \\ 1 \end{Bmatrix} \ddot{u}_g(t) \quad (2)$$

Rayleigh damping of 5% damping ratio is adopted, the mass proportional coefficient a_0 (1/sec) and stiffness proportional coefficient a_1 (sec) are calculated based on carefully selected natural frequences of the studied buildings which extracted from the first, second and third mode shapes.
The structural software ETABS Ultimate C (Version 20.3.0 Build 2929) has been used to perform the nonlinear time history analysis of moment resistance frame building models. In terms of material and geometrical nonlinearities, nonlinear analysis is considered as a realistic structural analysis that can imitate the appropriate behaviour of the material and the deformation of structural elements under dynamic loads. The performed nonlinear TH analyses herein employed Takeda hysteresis model. This model follows hysteretic rules for describing the nonlinear relation between the applied force and the corresponding deformation of the structural members. The figure illustration of the Force displacement relationships of Takeda hysteretic model is shown in Fig. 3. The concrete and rebar properties used in analysis are shown in Fig. 4. Beam-column element's both ends have plastic hinges (flexural hinges in beams, biaxial axial-flexural hinges in columns) have been used for the structural members of the nonlinear models. Mander stress–strain curve is assigned to concrete material section for confined and unconfined compression and tension stress–strain relation (Mander et al. 1988) [27].

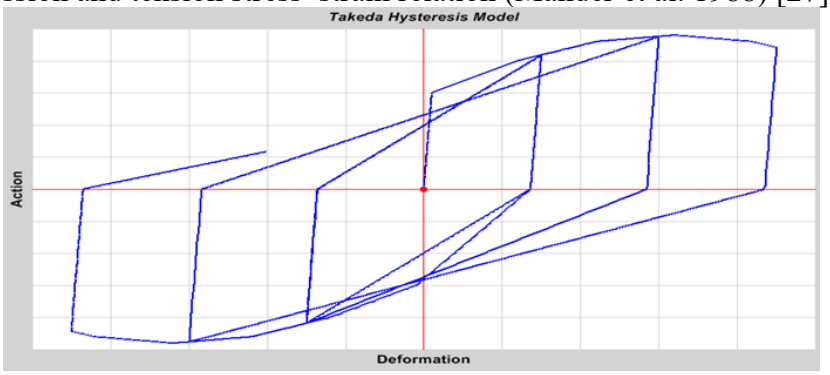

Fig. 3 Force-deformation relationship for Takeda hysteresis Model developed in ETABS.

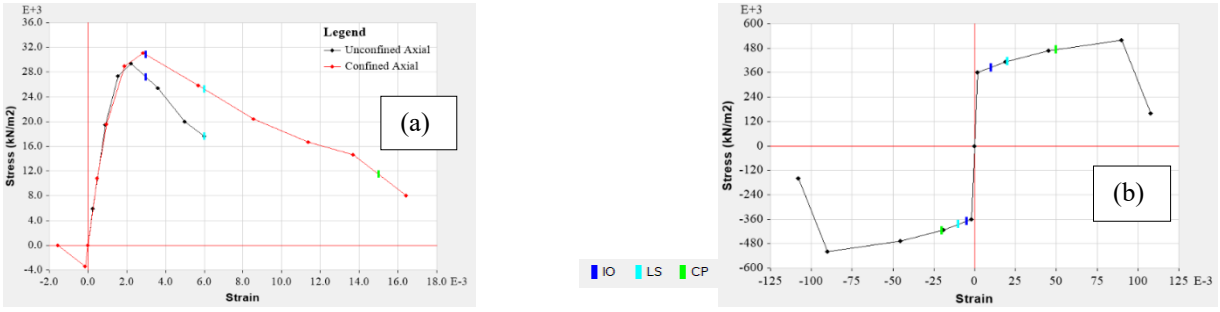

Fig. 4 Nonlinear stress strain curve for (a) concrete and (b) steel rebar used with acceptance criteria (IO, LS, and CP) on each curve.

The yielding and post-yielding behaviour can be modelled using plastic hinges. Hinge properties can be computed automatically from the element material and section properties according to FEMA-356 (FEMA 2000) [24] or ASCE 41-17 criteria (ASCE 2017) [25]. The fiber P-M2-M3 hinge models the axial behaviour of a number of representative axial fibers distributed across the cross section of the frame element.

3.2 Nonlinear pounding model assumptions

To simulating induced pounding force among adjacent structures, the gaps between the buildings are modelled by using compression only gap element as shown in Fig. 5. The pounding force of impact model $\overline{F}_P$ is determined as:

$$\overline{F}_P = \begin{cases} k\delta + c\dot{\delta}, & \delta \geq d \\ 0 & , \delta < d \end{cases} \quad \delta = u_i - u_j - d \,, \dot{\delta} = \dot{u}_i - \dot{u}_j \tag{3}$$

where δ and $\dot{\delta}$ indicate the relative displacement and velocity between colliding building elements. c, k, $\dot{u}_i$, $\dot{u}_j$, u_i, u_j and, d are the damping, stiffness, displacement, velocity of the element's nodes i, j and d is the separation gap for the impact model, respectively.
Different approaches to estimate the gap element stiffness have been examined in several studies. Based on the theory of wave propagation, Watanabe and Kawashima [28] conducted a mathematical model to determine the appropriate impact spring stiffness and the numerical integration time interval. Maison and Kasai [29] concluded that the impact stiffness can be described as the contact bodies' axial stiffness, and that a gap element with a stiffness equal to the floor's axial stiffness at the impact level is integrated. Gap element with a 20x amplification factor times the rigid SDOF system's lateral stiffness was presented [30]. At the present research, the gap element's impact stiffness "k" is calculated as the higher value of stiffer building's lateral stiffness at the impact level or the impacted floors' axial stiffness according to Eq.4. [31, 32].

$$k = \gamma \frac{EA}{b} \qquad or \qquad \gamma = \frac{3EI}{h^3} \tag{4}$$

where, A is the impact surface, E is the elasticity modulus, and b is width of building in the impact direction, I is the stiffer building's moment of inertia as equivalent cantilever model, h is the building height till the level of impact. The stiffness amplification factor, γ = 50 is calculated based on a sensitivity study of the impact stiffness value. The damping constant c is used to account for energy dissipation during colliding. However, the acceleration response may be strongly influenced by overly large values of spring stiffness and may compromise the precision of the dynamic model response. The impact element uses the damping component to take into consideration how much energy is dissipated through each colliding. Reasonable values of this coefficient can be calculated by comparing it to the restitution coefficient, e, for two masses, m_x and m_y, colliding with arbitrary velocities [30].

$$c = 2\xi\sqrt{k\frac{m_x m_y}{m_y + m_y}} \quad \text{and} \quad \xi = \frac{-\ln e}{\sqrt{\pi^2 + (\ln e)^2}} \tag{5}$$

The restitution coefficient varies from zero to one, which represents completely plastic impact to elastic impacts, respectively. A restitution coefficient of 0.65 (ξ = 0.14) has been used for structures impact involving concrete-to-concrete collisions [30,33,34].

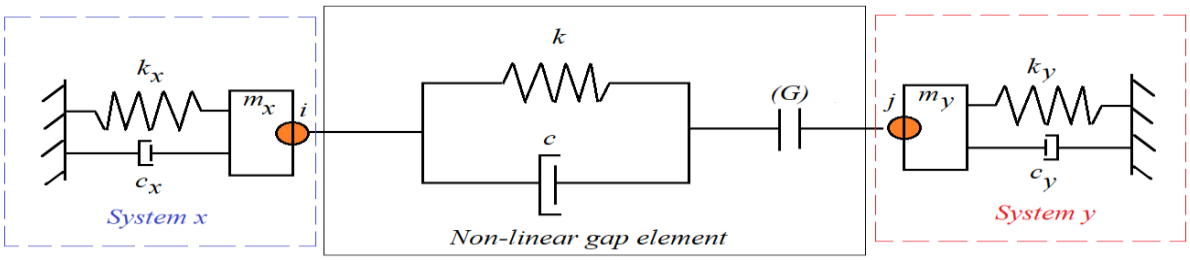

Fig. 5 Nonlinear gap element impact model between adjacent buildings

4. Physical building model and ground excitation

A group of strong ground excitation that are used as acceleration inputs to neighbouring structures is described in this section, along with the parameters of those structures. This section also includes the response parameters of the energy balance. The following subsections include the details of these parameters.

4.1 Physical building model

The building construction industry in Egypt had broadly used medium-rise RC buildings having twelve stories, the height limit authorized by the local authorities in most regions. These buildings are constructed with diverse patterns and structural systems. In the present study three models for typical buildings with three, six and twelve stories are selected as depicted in Fig. 6. The buildings have story height 3 m for all floors and bay width 5 m in each direction. Concrete with compressive strength f_c = 30 MPa, unit weight = 25 kN/m^3, modulus of elasticity E_c = 24 GPa, Poisson's ratio υ = 0.2 and reinforcing steel with yield strength F_y = 360 MPa are used for analysis and design. The dead loads take account of the own weight of the structural components; the weight of flooring cover (1.5 kN/m2) and panel wall loads intensity of 10 kN/m on all beams. A live load of 2 kN/m^2 is selected for the residential buildings. The floor has 0.15 m slab thickness and 0.3 × 0.7 m dropped beam with equally top and bottom reinforcement 5T12 and 5T8/m confinement stirrups. The dimensions and reinforcement of column elements for the studied buildings are presented in Table 1. The practice on buildings subjected to earthquakes shows that masonry infill walls completely modify the behaviour of bare frames due to increased initial stiffness and low deformability, but it is difficult to predict the masonry infill effect on the frames members, as different failure modes can occur either in the masonry or in the surrounding frame. Thus, due to several uncertainties regarding the infill layout as non-structural elements, openings through infill wall, complications in modelling infill wall-frame interaction, the infill effects are hard to be quantified and usually ignored in structural design (Elwardany et al. 2017) [7]. The capacity design rules are adopted, where the brittle failure or other harmful failure mechanisms (plastic hinges in columns, shear failure of structural elements, failure of beam-column joints, yielding of foundations) shall be prohibited, through definition of the design actions through selected regions from equilibrium conditions, such that plastic hinges with their possible over-strengths have been created in their adjacent areas (ECP 2008) [37]. For the MRF structural systems, the capacity design condition should be fulfilled at all beam-column joints.

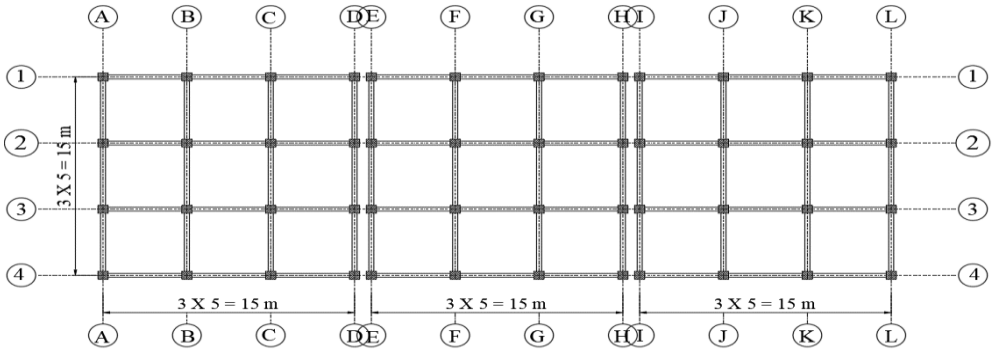

(a)

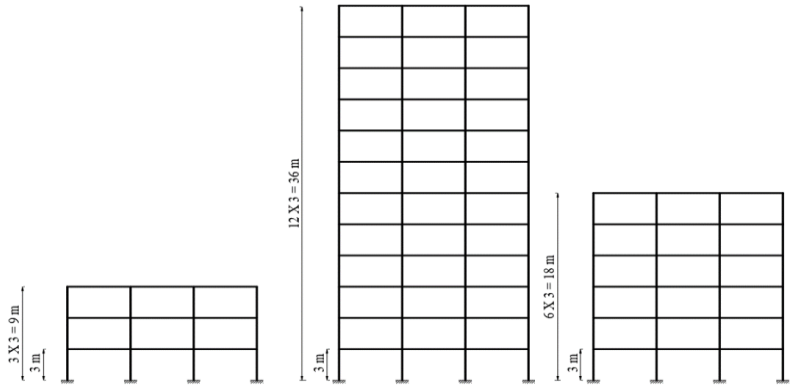

(b)

Fig. 6 Three-, six- and twelve-story buildings: a) typical floor plan, b) elevations

Table 1 Cross-sections dimension (mm) and rebar for column of the building model

Building	Column location	Story No.			
		From 1 to 3	From 4 to 6	From 7 to 9	From 10 to 12
		Dimension Reinforcement	Dimension Reinforcement	Dimension Reinforcement	Dimension Reinforcement
12-Story	Corner	600 × 600 26T20	500 × 500 22T18	500 × 500 22T14	400 × 400 22T14
	Edge	700 × 700 26T20	600 x 600 22T20	500 × 500 22T18	400 × 400 22T14
	Interior	800 × 800 30T22	700 x 700 28T22	600 × 600 26T20	500 × 500 22T20
6-Story	Corner	500 × 500 22T14	400 x 400 22T14		
	Edge	500× 500 22T18	400 x 400 22T14		
	Interior	600 × 600 26T20	500 x 500 22T20		
3-Story	Corner	400 × 400 22T14			
	Edge	400 × 400 22T14			
	Interior	500 × 500 22T18			

4.2 Ground excitations.

The current research uses two ground excitation that are shown in Table 2 which are employed as acceleration inputs to the three adjacent buildings. one of these ground motion has been taken from far-fault region El Centro 1940 (Imperial Valley) [35], and the other has been taken form near-fault 1995 Kobe earthquakes. Table 3 list important parameters on above mentioned input excitations, like, station of recording, soil classification, magnitude, peak ground acceleration (PGA), distance from source to stie, and total duration. With varying PGA, distinct frequency content, total duration (10 and 20 s) and soil class, both near-fault and far-fault records represent strong different ground motion. Plots of the ground acceleration time-histories and corresponding Fourier amplitude spectra for each of these records are represented in Fig. 7. With a site-source distance of roughly 0.6 and 8.3 kilometers, the earthquakes have magnitudes of 6.9 and 7.2. The two ground excitations are applied separately in the pounding direction.

Table 2 Strong ground motion records used as input to adjacent buildings.

Earthquake (record)	Date	Soil Class	Station	PGA (g)	*M*	D_{ss} (km)	t_d (s)
El Centro (180)	05.19.1940	D, C	117 El Centro	0.34	7.2	8.3	53
Kobe (000)	01.16.1995	B, B	0 KJMA	1.00	6.9	0.6	48

Soil class = geomatrix soil class, USGS, PGA = peak ground acceleration, *M* = magnitude, D_{ss} = site–source distance, t_d = earthquake total duration.

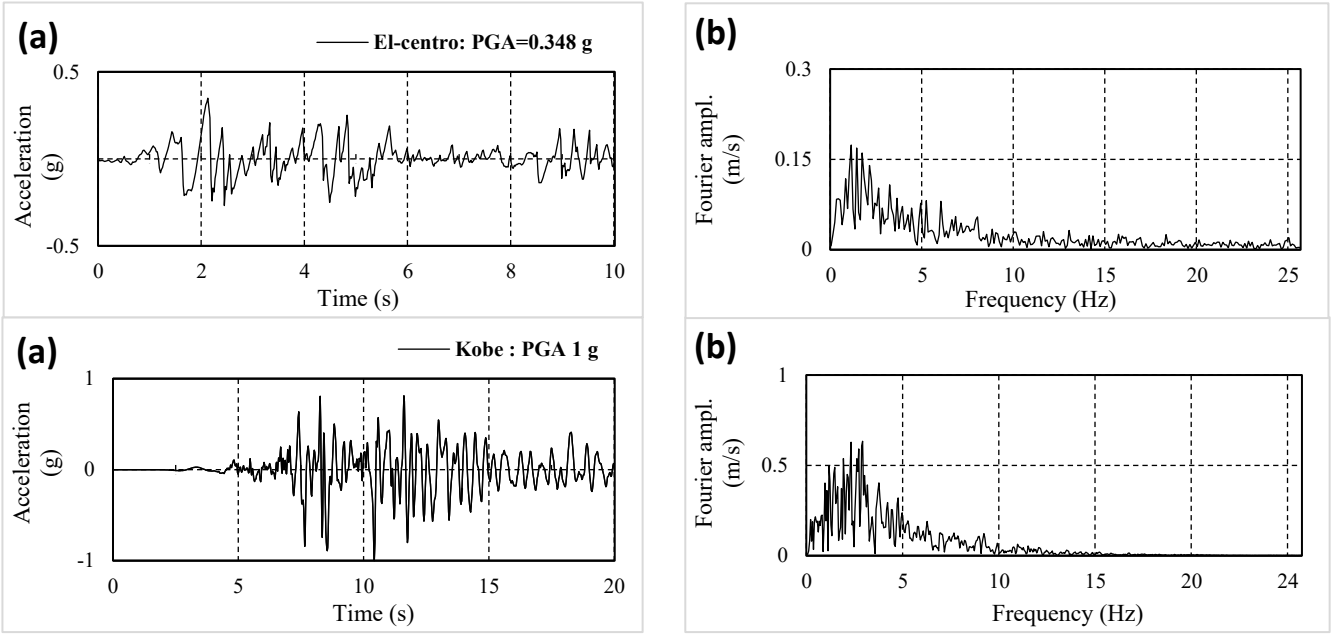

Fig. 7 Ground excitation record to adjacent structures (a) Acceleration time histories (b) Fourier amplitude

5. Numerical results and discussion

To guarantee the response of the three buildings being inelastic, all acceleration time histories records in numerical analysis shall be scaled to 1.00 g PGA. The gap distance named "d" is taken equal to different values such zero (case of full contact), 0.05, 0.10, 0.15, 0.20, and 0.25 m. In addition to gab distance is bigger than maximum amplitude (d_{max}. A_{mpl}) i.e. the buildings are considered fully separated by each other (standalone buildings). The adjacent structures configuration is displayed at Fig.8.

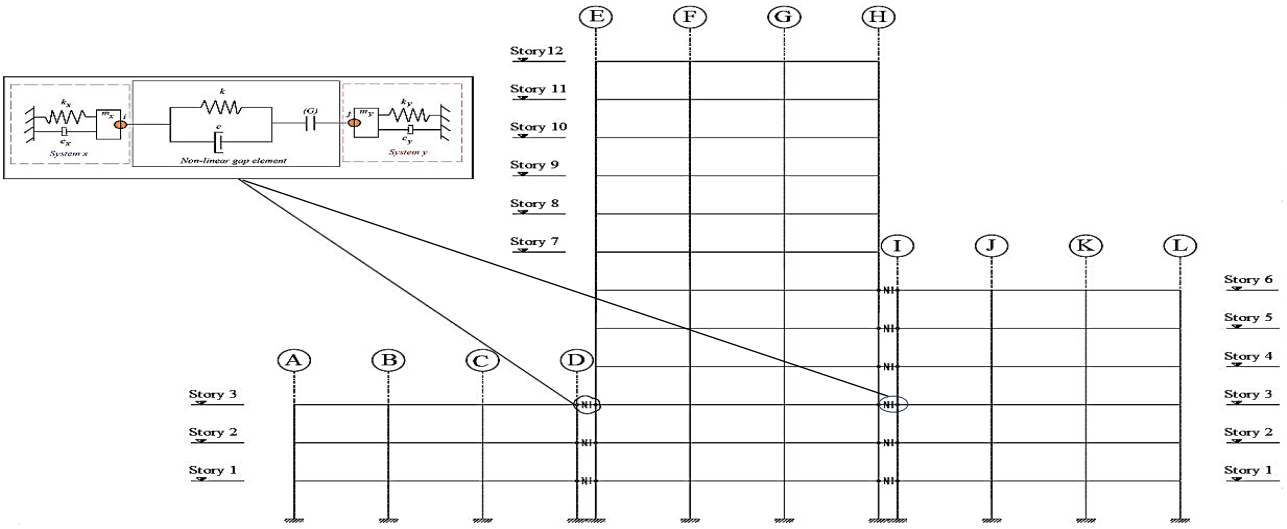

Fig. 8 Buildings system alignment configuration

5.1 Analysis of natural vibration of buildings

The fundamental natural time period and frequency of structures can be estimated by either using experiments methods or using analytical modelling. Each building has its own dynamic characteristics that basically rely on its stiffness, mass, and damping. The buildings will vibrate at their inherent frequency if they are allowed to do it freely without interference from any external loads such induced pounding force. Table 3 lists the fundamental periods for first three mode shapes (dominated mode shapes) as determined by finite element model and approximate formulas in the earlier and older version of Egyptian Code Participate [36, 37] in addition to internationals codes.

Table 3. fundamental natural time periods for different buildings model to perspective vibration mode

Building code	Equation / mode shape	Fundamental period (s)		
		12-Story	6-Story	3-Story
3D FE model	1st lateral vibrat1ion mode shape	1.522	0.878	0.523
	2nd lateral vibration mode shape	0.546	0.314	0.173
	3rd lateral vibration mode shape	0.318	0.178	0.113
EC8 [39]	$T_1 = C_{0.075}H^{3/4}$	1.102	0.655	0.390
ECP-201 [36]	$T = 0.075H^{3/4}$	1.102	0.655	0.390
ECP-201 [37]	$T = 0.1\,N$, N is the number of stories	1.200	0.600	0.300
FEMA 356 [24]	$T = 0.018\,h_n^{0.9}$,h_n height in feet	1.319	0.706	0.378
ASCE 7-16 [21]	$T_a = 0.016h_n^{0.9}$,h_n height in feet	1.172	0.628	0.336
	$T = 0.1\,N$, N is the number of stories	1.200	0.600	0.300
NBCC [38]	$T = 0.05\,H^{3/4}$	0.735	0.437	0.260

In comparison to those calculated from structural models based on 3D FE analysis, the calculated periods based on empirical formulas from building codes are substantially shorter. The adjacent structures models have fundamental periods of 1.102, 0.655, and 0.390 s based on ECP-201 [38], while the FE approach based on the first mode shape has fundamental periods of 1.522, 0.878, and 0.523 s. This amounts to 142, 134, and 134% for the 12-story, 6-story, and 3-story buildings that were introduced in the code provisions. Therefore, it is evident that the code empirical expressions were unable to present fundamental periods with adequate accuracy building models. The vibration period serves as the primary parameter for the dynamic characteristics of structures.

5.2 The impact of separation distance on the seismic response parameters

The nonlinear dynamic time history analysis has been performed for different gap distances; d= 0.05, 0.10, 0.15, 0.20, 0.25m in addition to in-contact pounding, d=0.00m. The responses parameter of different gap sizes compared with the case of full-separated buildings in which d > $d_{max.\ ampl.}$. Figures 9, 10 and 11 show the relative displacement of building's story at impact level and the corresponding induced pound force at in-contact adjacent building and gap distance of 0.05m to Kobe (000) and El Centro (180) ground motion records.

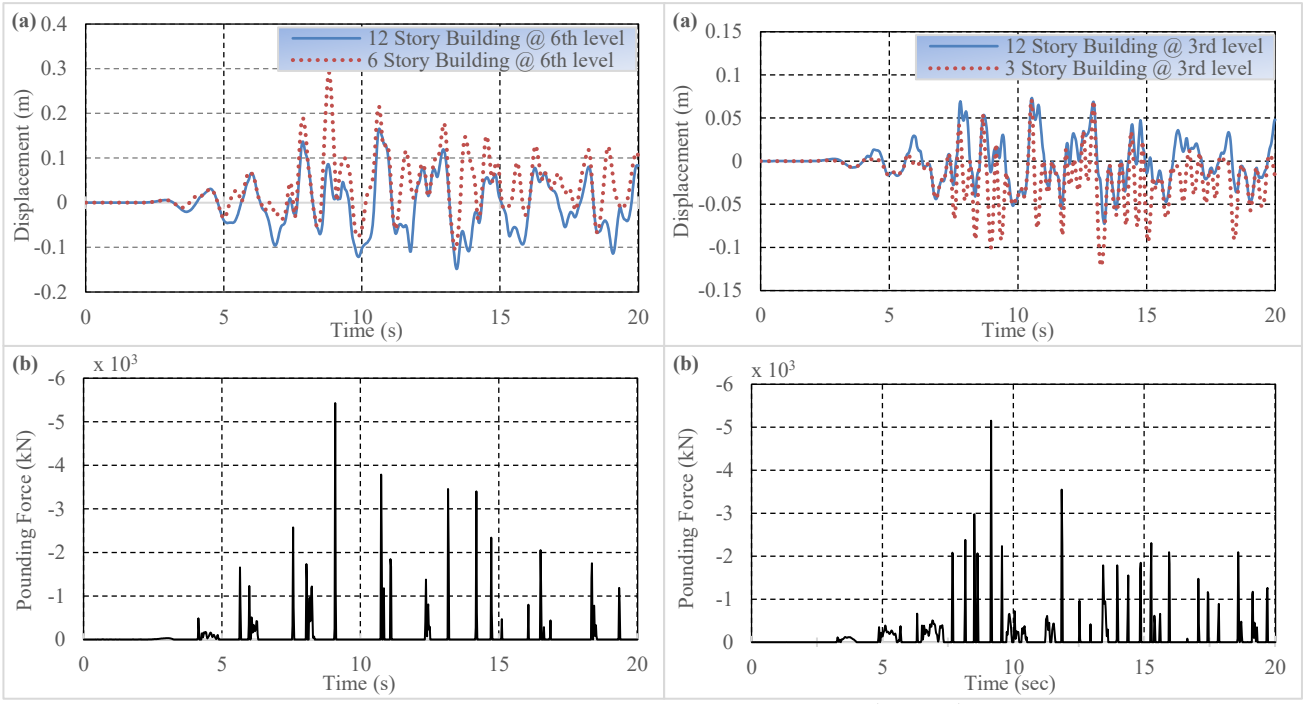

Fig. 9. Response parameters for 12 story,6 story and 3 story buildings at 3rd and 6th impact levels to Kobe (000) record (a) Displacements, (b) corresponding induced pounding force (d=0.00 m)

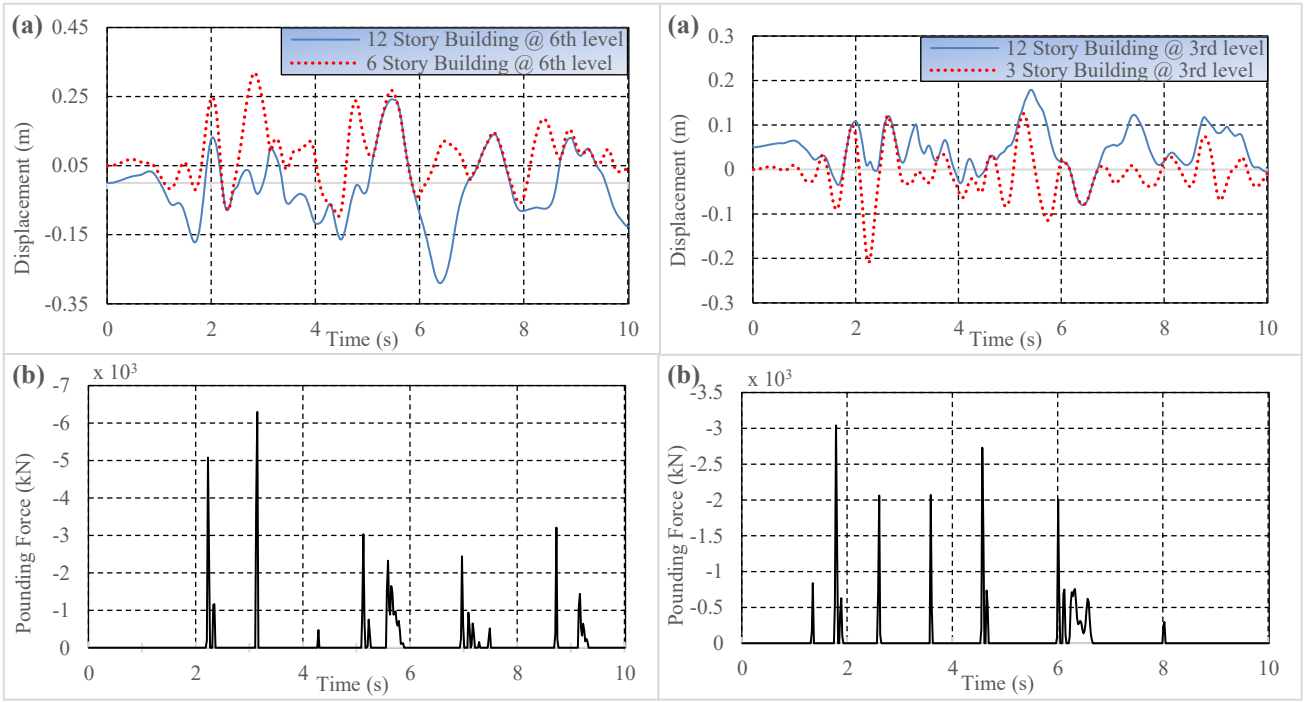

Fig. 10. Response parameters for 12 story,6 story and 3 story buildings at 3rd and 6th impact levels to Kobe (000) record (a) Displacements, (b) corresponding induced pounding force (d=0.05 m)

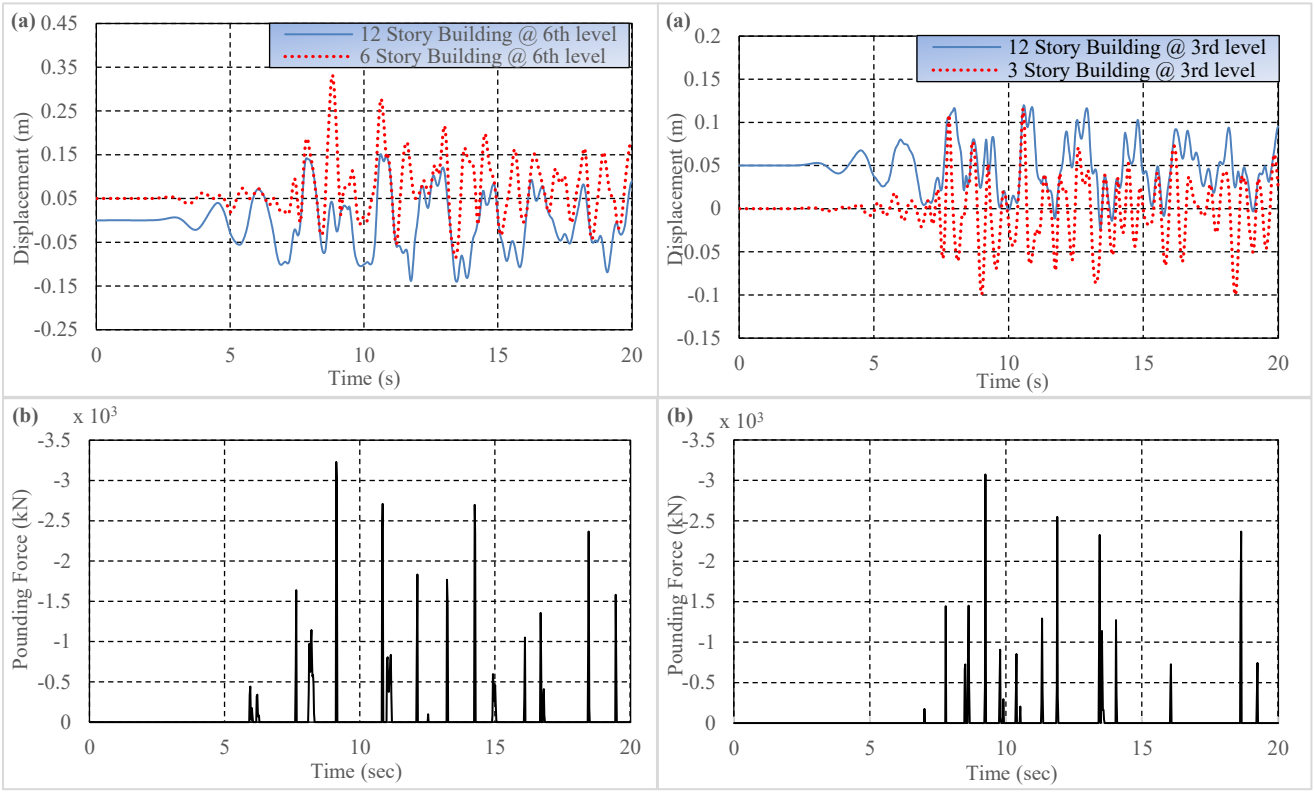

Fig.11 Response parameters for 12 story, 6 story and 3 story buildings at 6th and 3rd level to El Centro record (a) Displacements, (b) corresponding induced pounding force (d=0.05 m)

Table 4. Peak induced pounding force for different gap distance size under Kobe (000) record (kN)

Story no.	Pounding force between 3- and 12 story building				Pounding force between 12- and 6 story building					
	d= 0 cm	d= 5 cm	d= 10 cm	d= 15 cm	d= 0 cm	d= 5 cm	d= 10 cm	d= 15 cm	d= 20 cm	d= 25 cm
Story 6	-	-	-	-	5430.37	3230.42	2537.51	1962.69	0.00	0.00
Story 5	-	-	-	-	4170.84	3588.78	2494.72	0.00	0.00	0.00
Story 4	-	-	-	-	1583.27	2243.87	0.00	0.00	0.00	0.00
Story 3	5152.93	3073.99	2818.53	0.00	2833.53	928.14	365.72	0.00	0.00	0.00
Story 2	3453.96	1411.68	0.00	0.00	1158.22	0.00	0.00	0.00	0.00	0.00
Story 1	1927.18	0.00	0.00	0.00	744.96	0.00	0.00	0.00	0.00	0.00

Table 5. Peak induced pounding force for different gap distance size under El Centro (180) record (kN)

Story no.	Pounding force between 3- and 12 story building				Pounding force between 12- and 6 story building					
	d= 0 cm	d= 5 cm	d= 10 cm	d= 15 cm	d= 0 cm	d= 5 cm	d= 10 cm	d= 15 cm	d= 20 cm	d= 25 cm
Story 6	-	-	-	-	4081.51	6295.45	5119.76	4206.75	4820.73	1890.08
Story 5	-	-	-	-	3182.73	3277.94	2893.74	4327.90	3118.60	0.00
Story 4	-	-	-	-	2510.80	2988.63	1710.77	0.00	0.00	0.00
Story 3	3147.69	3039.10	1864.84	0.00	2669.60	1545.19	0.00	0.00	0.00	0.00
Story 2	2258.12	733.94	0.00	0.00	1657.75	0.00	0.00	0.00	0.00	0.00
Story 1	883.37	0.00	0.00	0.00	735.26	0.00	0.00	0.00	0.00	0.00

Tables 4 and 5 represent the peak induced pounding force under Kobe (000) and El Centro (180) records for different gap distance of 0.05, 0.10, 0.15, 0.20, 0.25 m and in-contact pounding. The table confirm that the induced pounding forces under Kobe (000) record are higher in magnitude than those induced under El Centro (180) for the forces induced between 3- and 12 story building for all gap distances and only for in-contact between 12- and 6 story building, otherwise the opposite is true. The pounding between 12-story building and 6-story buildings at 6th story level displays higher value of the impact force for gap size d = 0.05 cm, even greater than the case of in-contact d = 0.00m especially for the

higher stories under El Centro (180) record. Furthermore, the potential impact is extended over all stories for the in-contact case, with lighter impact at lower stories under both input excitation. While the maximum induced pounding force located at 3rd story between 3- and 12 story building and 6th story between 12- and 6 story building found at case of in-contact under Kobe (000) record. Furthermore, the pounding force magnitude decreases with increase of separation distance especially at higher stories. The effect of induced pounding force vanishes at gap distance of d = 0.15 m for all stories between 3- and 12 story building under both input excitation which indicates that pounding has no effect on adjacent buildings response. However, under the El Centro (180) record, the response between a 12- and 6-story building is affected by the induced pounding force until the gap distance of d = 0.25 m. The frequent number of powerful collisions and the impact force magnitude both influence the possible damage from pounding (see figures 10, 11, and 12). Different floor levels may experience pounding, which enables the activation of several contact points along the buildings' height. The figures also demonstrate that the number of impact occurrence inversely proportional to the gap distance between adjacent buildings.

Fig.12. presents Maximum story displacement response along building height of different gap distances for adjacent building under Kobe (000) and El Centro (180) records which confirms the influence of pounding on the story displacement responses curve of the adjacent building. The maximum story displacement relies on the input ground motion characteristics and the size of gap distance. The envelops confirms that, as the width of separation gap get expanding, the pounding between the adjacent building most likely to be eliminated. Under Kobe (000) input excitation, the gap distance of 0.15 m is sufficient to significantly eliminate the colliding effect between the adjacent building. While a gap distance of more than 0.25m is required to eliminate the pounding effect between the adjacent buildings under El Centro (180) records. On the impact side, seismic pounding restricts story displacement, but it can also increase story displacement responses on the other side (rebound side). This is especially true for a 3-story building with a gap distance of 0.05 m under El Centro (180) and in contact case under Kobe (000) records. The pounding effect of the impact at the 6th level between the 12- and 6-story buildings is more significant than that of impact at 3rd level between 12- and 3-story buildings. The effect of El Centro (180) records on the peak displacement is more powerful than Kobe (000) records.

Figures 13, 14, 15 and 16 present the hysteretic loops (in moment-rotation formula) of bottom plastic hinge of ground floor edge columns comparing between pounding and no-pounding case under El Centro (180) earthquake for the three adjacent buildings. Studies of damage from previous major earthquakes show that the pounding phenomenon can cause significant damage for particular structural elements or even complete failure of buildings if the distance between them is not large enough. The building collision lead to change the building's fundamental response to ground movements and transfers additional inertial loads and energy from the adjacent structure to the others. From of particular concern is the possibility of extreme localized damage to structural elements in the region impact zones. The analysis of the energy balance confirms that the collision, beside the Local damage, it may cause increase or decrease the response of adjacent building based on the natural vibration characteristics of adjacent buildings. Comparisons between cases with and without pounding show that structural pounding can significantly boost the magnitude and level of damage. The results from figures 13 (b) and 14 (a) under Kobe (000) earthquake record show that collisions lead to a significant increase of the rotations value of the higher building as well as may result in a substantial increase of the range and intensity of damage at the base of building especially for col. 34 and 46. The max (+ve) rotation value of column 34 of 12-story building is increased by approximately 300% for the pounding case compared to no-pounding case. The Fig.15 (a) for shorter building explicitly confirm that, the rotation value reduced significantly; therefore, the pounding severity is reduced (for col. 62). The max (+ve) rotation value of column 62 of 3-story building is decreased from 0.03 rad to 0.02 rad.

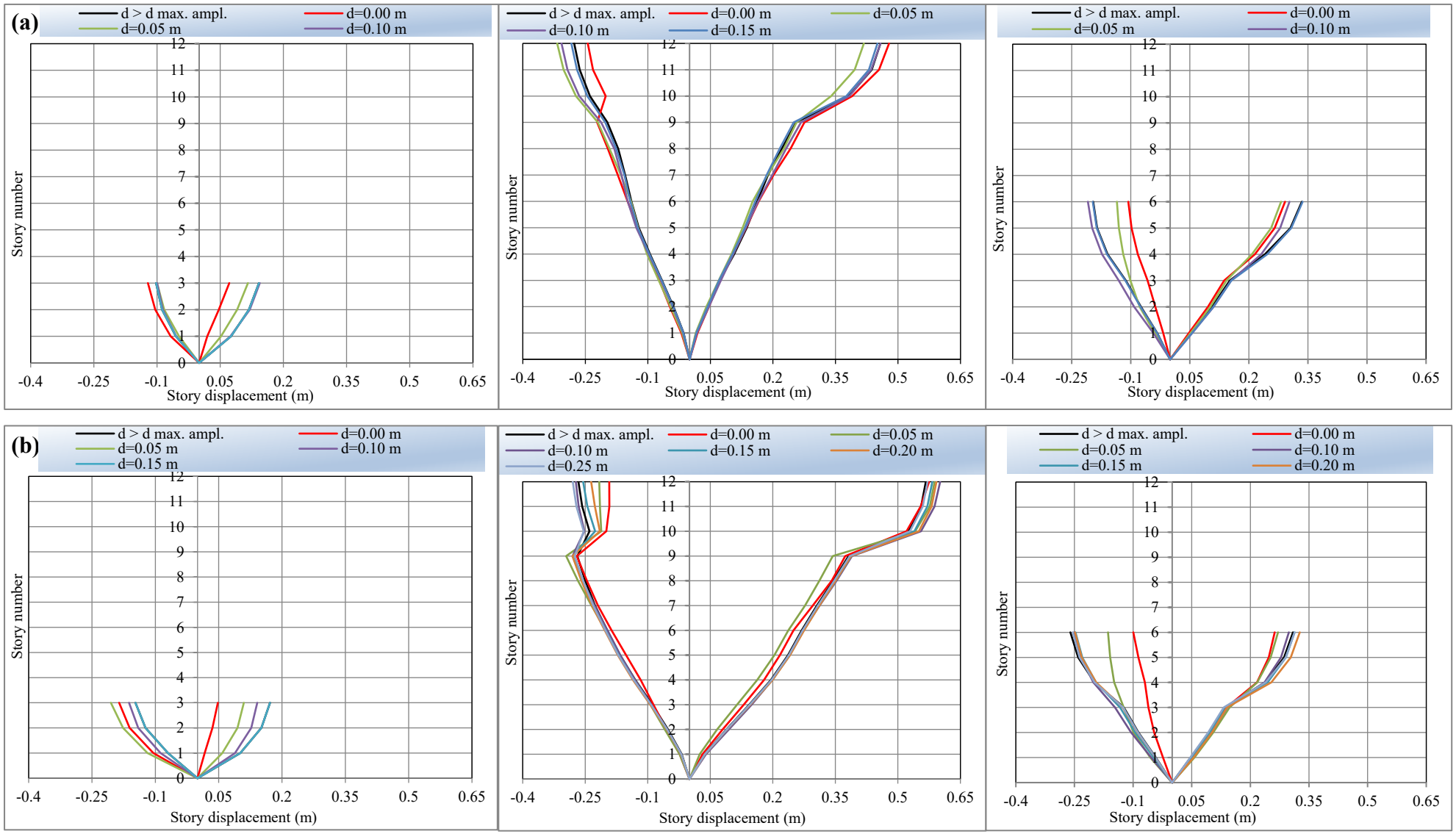

Fig12. Maximum story displacement response along building height of different gap distances for adjacent building under (a) Kobe (000) record (b) El Centro (180) record

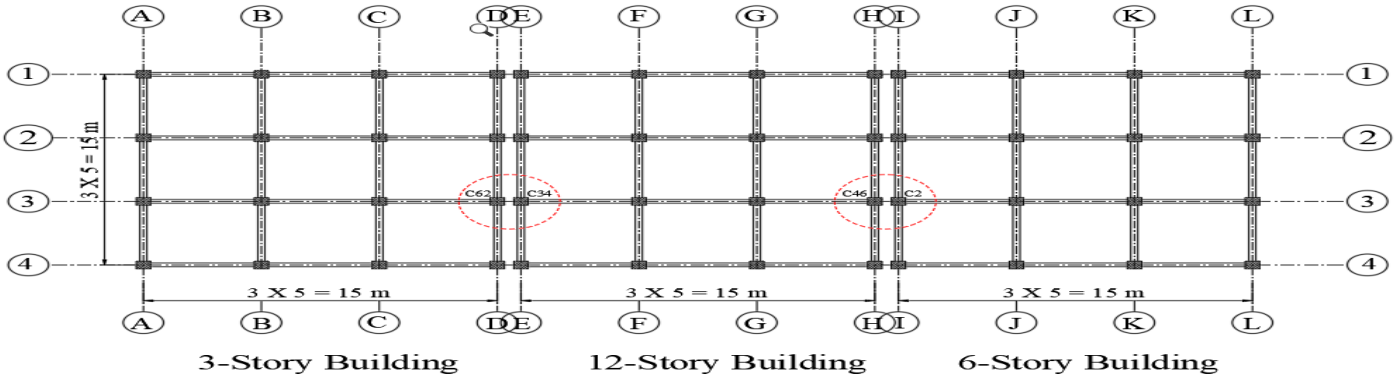

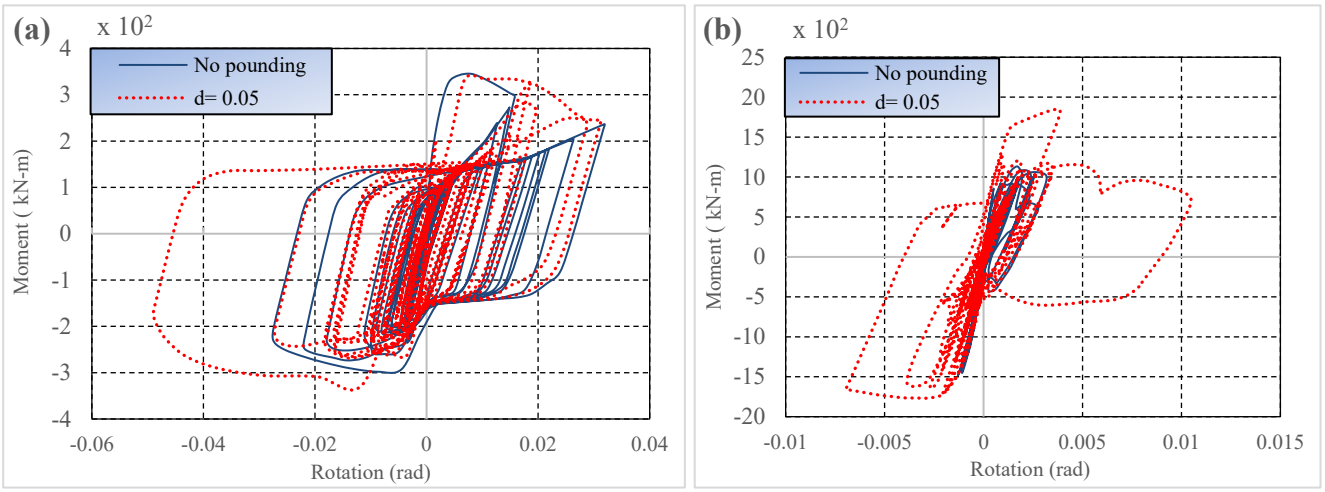

Fig. 13. Hysteretic loops of bottom plastic hinge of ground floor column for pounding (d=0.05m) and no-pounding case under El Centro (180) earthquake (a) column 62 of 3-story building (b) column 34 of 12-story building.

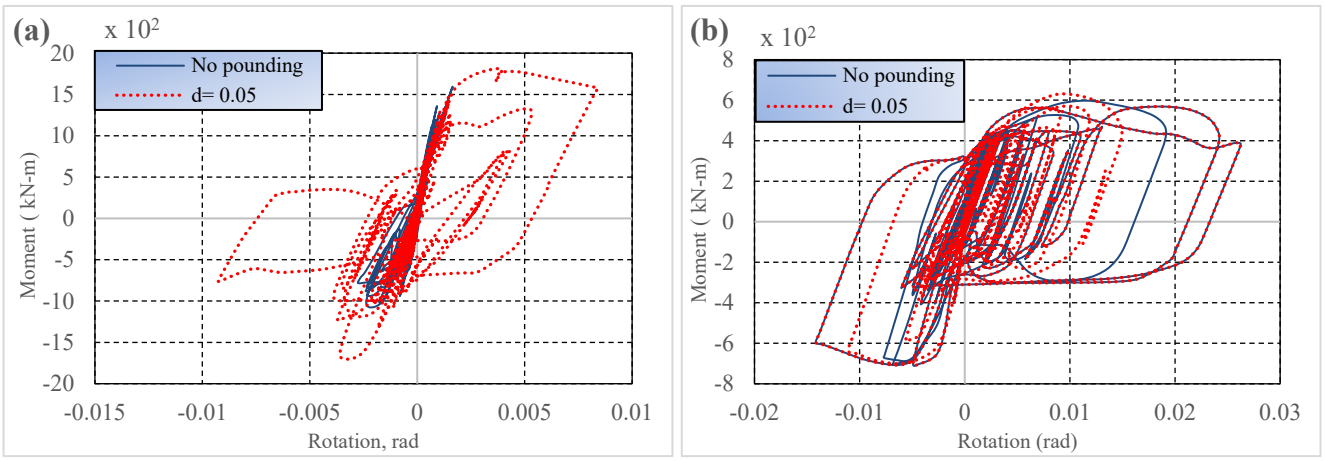

Fig. 14. Hysteretic loops of bottom plastic hinge of ground floor column for pounding (d=0.05m) and no-pounding case under El Centro (180) earthquake records (a) column 46 of 12- story building (b) column 2 of 6- story building

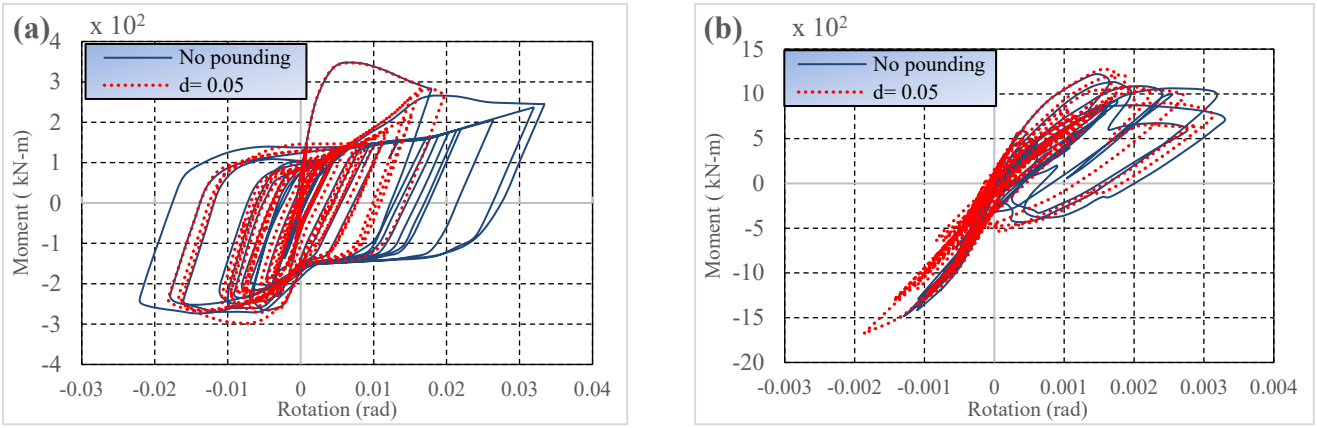

Fig. 15. Hysteretic loops of bottom plastic hinge of ground floor column for pounding and no-pounding case under Kobe (000) earthquake records (a) column 62 of 3-story building (b) column 34 of 12-story building.

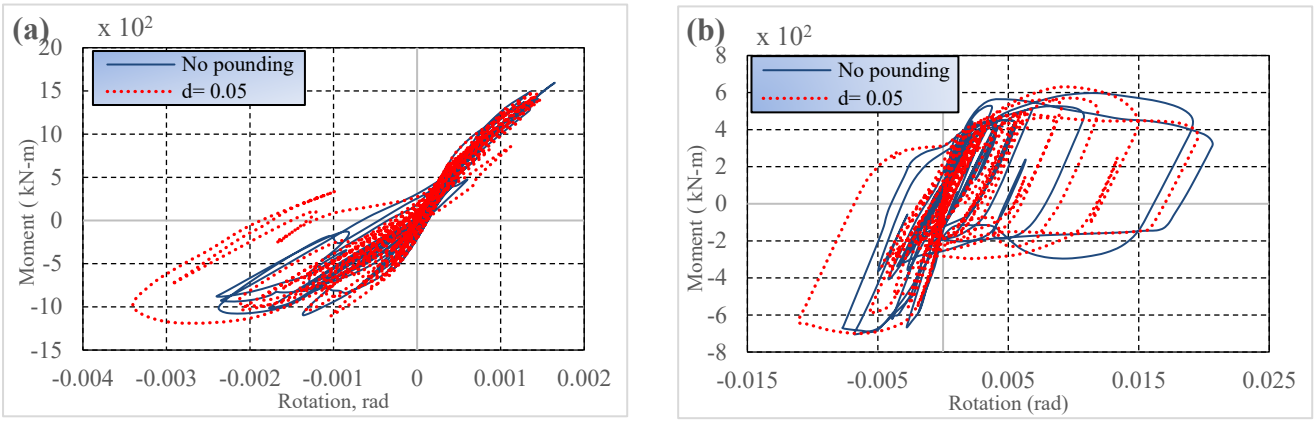

Fig. 16. Hysteretic loops of bottom plastic hinge of ground floor column for pounding and no-pounding case under Kobe (000) earthquake records (a) column 46 of 12- story building (b) column 2 of 6- story building.

Figure 17 show acceleration time histories of adjacent building at top level of shorter buildings (3-story and 6-story buildings), under Kobe (000) earthquake record for gap distances of 0.00 and 0.05 m in addition to case of no-pounding. Collisions between adjacent structures intensify the acceleration response, which might increase by multiple times in comparison to the case of no pounding. The most noticeable alteration in figures is the increase in both direction whenever accelerations are positive and negative for the 12-story building (the middle building) due to two-sided impacts, while there are spikes in negative accelerations for the 3-story building and spikes in positive accelerations for the 6-story building because of the configuration arrangement (one-sided impact).

Table 6 demonstrates the maximum values of acceleration at the impact level of 3-story and 6-story buildings under Kobe (000) and El Centro (180) records for different gap distances and compared to the fully separated case. The size of the gap distance and the input ground motion characteristic affect the peak acceleration responses. Both edge buildings (3-story and 6-story buildings) are exposed to one-sided impact, and typically, this result in a very significant acceleration magnification in the rebound direction, which can reach 492% at the 3rd level of impact and 616% at the 6th level of impact. On the contrary, the inner building (12-story building) is subjected to two-sided impacts, which results in significant acceleration magnification, which can reach 329% at the 3rd level of impact and 603% at the 6th level of impact. For the full contact case, the maximum acceleration in the negative direction at the 3-story building's top level is -68.54 m/s^2 at 9.14 sec. It is approximately four times higher than the non-pounding case, which is just -17.14 m/s^2 at 11.07 s. The maximum acceleration in the positive direction generated at a 6-story building's top level under Kobe (000) excitation is 73.27 m/s^2 at 9.08 sec., while

the corresponding max. value El Centro (180) record is 65.91 m/s^2 for a gap distance of 0.05 m. It is approximately four to six times greater than the non-pounding case which is just 10.69 m/s^2.

Table 6. Peak acceleration response at impact level under Kobe (000) and El Centro (180) records (m/s^2)

Earthquake / pounding condition	Impact between 3- and 12-story buildings				Impact between 12- and 6-story buildings			
	3-Story building		12-Story building		6-Story building			
	Impact at 3rd level				Impact at 6th level			
	Rebound	Impact direction		Rebound	Rebound	Impact direction		Rebound
Kobe (000)								
No pounding	-17.14	16.89	-12.51	12.17	-17.42	16.36	-19.55	16.71
Pounding d = 0.00	-68.54	19.55	-24.94	33.25	-40.08	23.60	-15.92	73.27
Pounding d = 0.05	-41.21	18.39	-30.51	26.21	-28.25	18.77	-16.31	52.40
El Centro (180)								
No pounding	-8.66	14.06	-5.89	9.36	-7.26	9.13	-12.00	10.69
Pounding d = 0.00	-42.57	13.11	-40.07	30.79	-35.25	20.28	-11.64	39.87
Pounding d = 0.05	-33.53	22.03	-36.87	22.12	-43.81	29.49	-17.34	65.91

Figure 18 presents the maximum horizontal story accelerations for different gap different gap distances with the case of standalone (fully separated) buildings under Kobe (000) and El Centro (180) earthquake records. It is evident from envelopes that structures exposed to pounding typically produce greater story acceleration compared to fully separated buildings in which d > d $_{max.\ ampl.}$. Under Kobe (000) the full contact case (d=0.00 m) gives higher acceleration response for all adjacent buildings compared to other cases especially at the level of impact. The acceleration response of interior building (12- Story building) beneath the level of impact is substantially higher at each direction because of two-sided impact, the response gets its maximum values at impact level and with gap distance of 0.00 m and decrease effectively with the increase of gap size, while the response of the floors at above the impact level is slightly affected. Moreover, the maximum responses of exterior buildings (6-story and 3- story building) are substantially higher in the directions of rebound throughout the building's height however, the acceleration is marginally modified in the direction of impact because of a single-sided effect on the edge buildings of alignment building configuration. For the result under Kobe (000) input load the pounding effect on the response is slightly affected with the gap distance of 0.15 m while the pounding affects the acceleration response up to gap distance of 0.25 m under El Centro (180) input load.

Figure 19 demonstrate input, hysteretic, global damping and kinetic energy for 12 story, 6 story and 3 story adjacent buildings for gap distance of 0.00 m, 0.05 m, 0.10m, 0.15m and fully separated case (d > d $_{max.\ amp.}$) under Kobe (000) ground motion record. The input, global damping and hysteretic energy time histories envelops for in-contact case, gaps of d = 0.00 and d = 0.10 m display higher energy values versus time relative to case of full separated for the high-rise interior building (12-story building). Moreover, the envelope for gap of d = 0.15 m nearly matches with the envelope for full separated case (d > d $_{max.\ amp.}$) for all adjacent buildings (high and low-rise buildings). There are significantly different between the envelope of in-contact case and the envelope of full separation for input, global damping and hysteretic energy envelopes. On the contrary, the difference is slightly of same envelopes for kinetic energy envelopes. The amplification is nearly 34%, 26% and 50% in peak input, global damping and hysteretic energy response respectively of case of in-contact (d = 0.00 m) relative to full separation case under Kobe (000) for the high-rise building. While the same amplifications are 40%, 36% and 50% under El Centro (180). For the low-rise exterior building (6- story building and 3- story building) the behaviour is completely opposite in which the input, global damping and hysteretic energy time histories envelop for in-contact case, gaps of d = 0.00 and d = 0.10 m display lower energy values versus time relative to case of full separated building. The reduction in peak input peak input, global damping and hysteretic energy response of case of in-contact (d = 0.00 m) relative to full separation case is nearly 35%, 30% and 46% respectively relative to full separation case under Kobe (000) for the low-rise building 6- story building. While the corresponding reduction is 49%, 35% and 62 % for the low-rise building 3- story building.

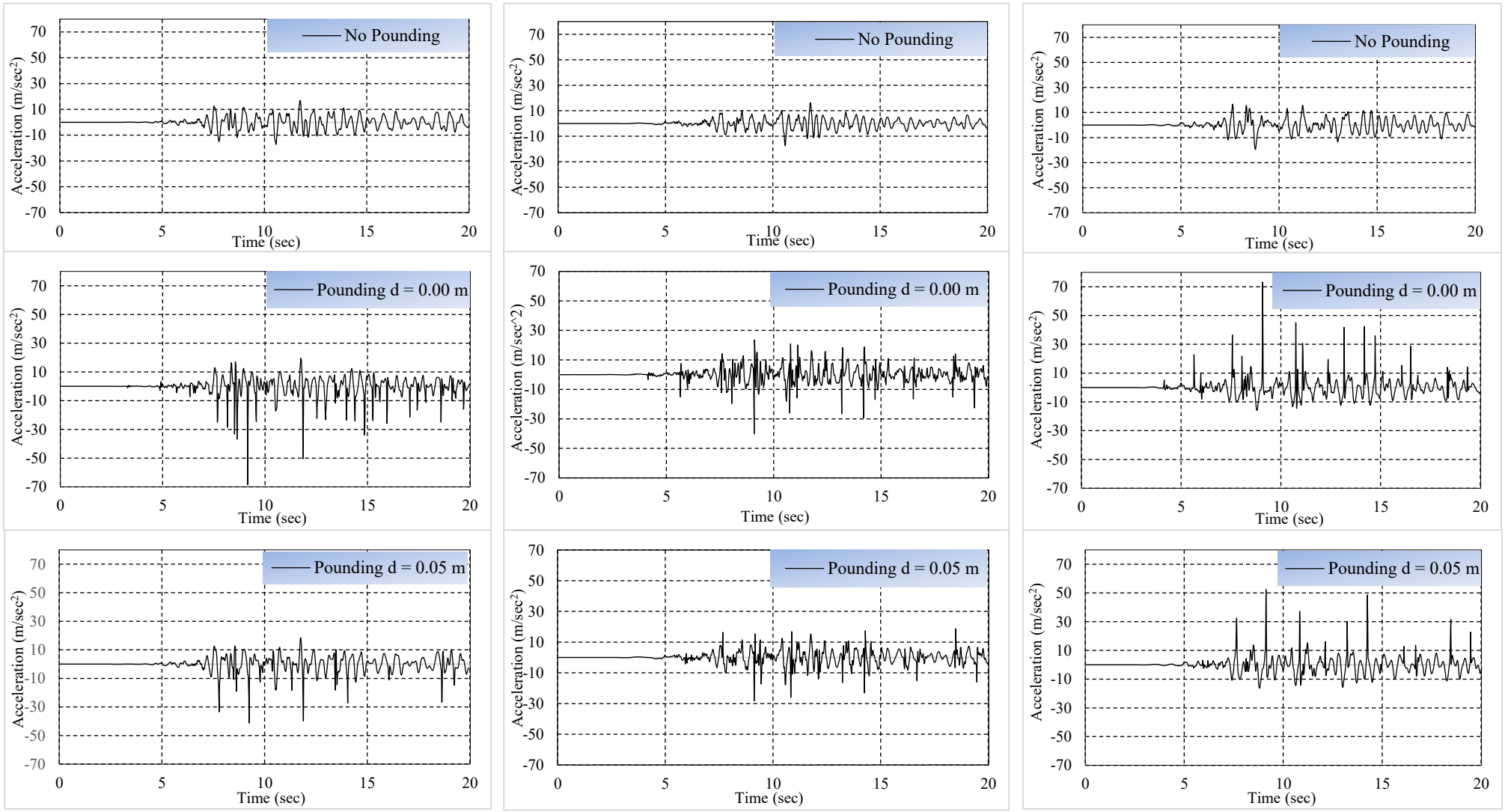

Fig. 17. Story acceleration time histories under the Kobe (000) earthquake record for different gap size

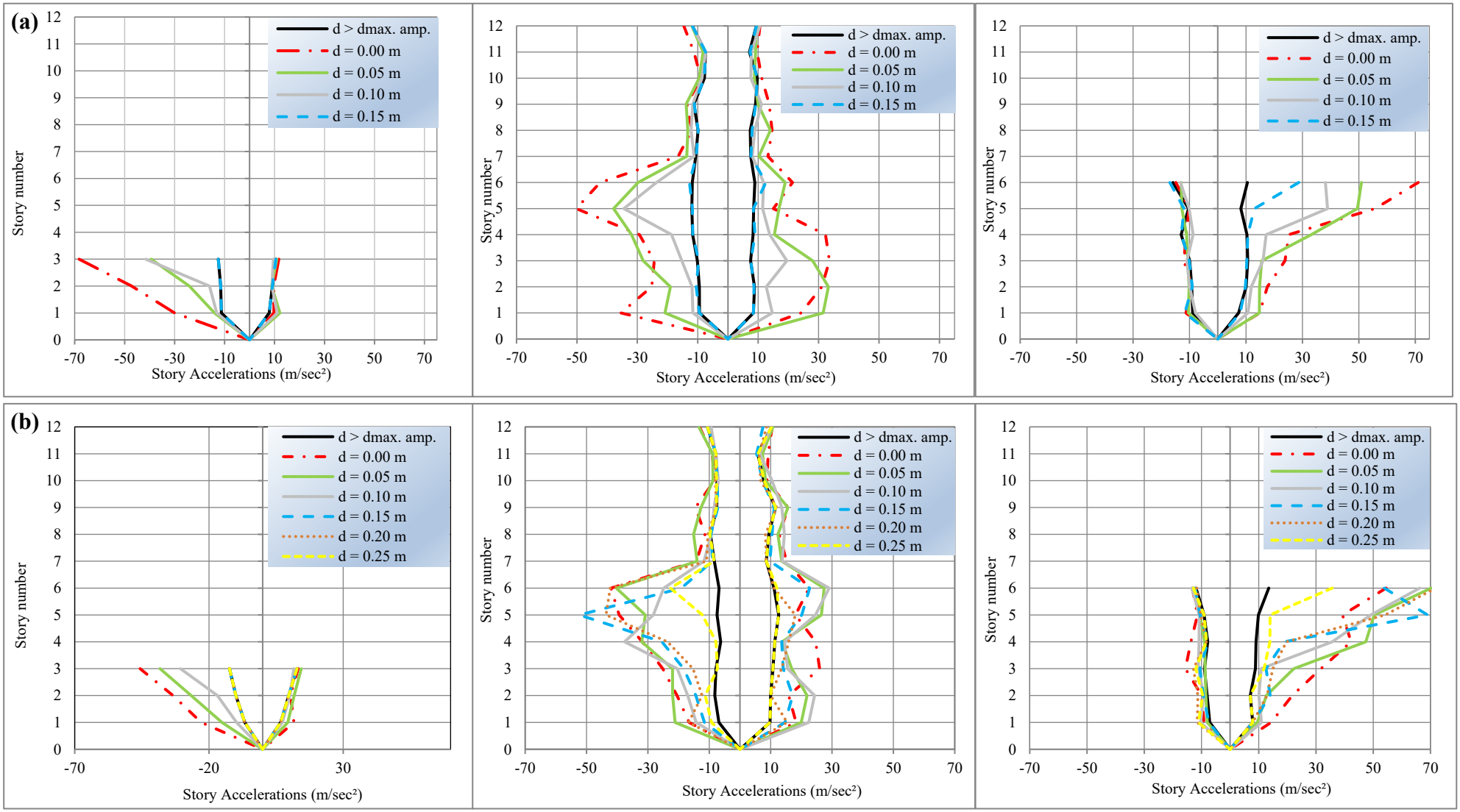

Fig. 18 Maximum story accelerations for different gap different gap distances under (a) Kobe (000) (b) El Centro (180) earthquake record

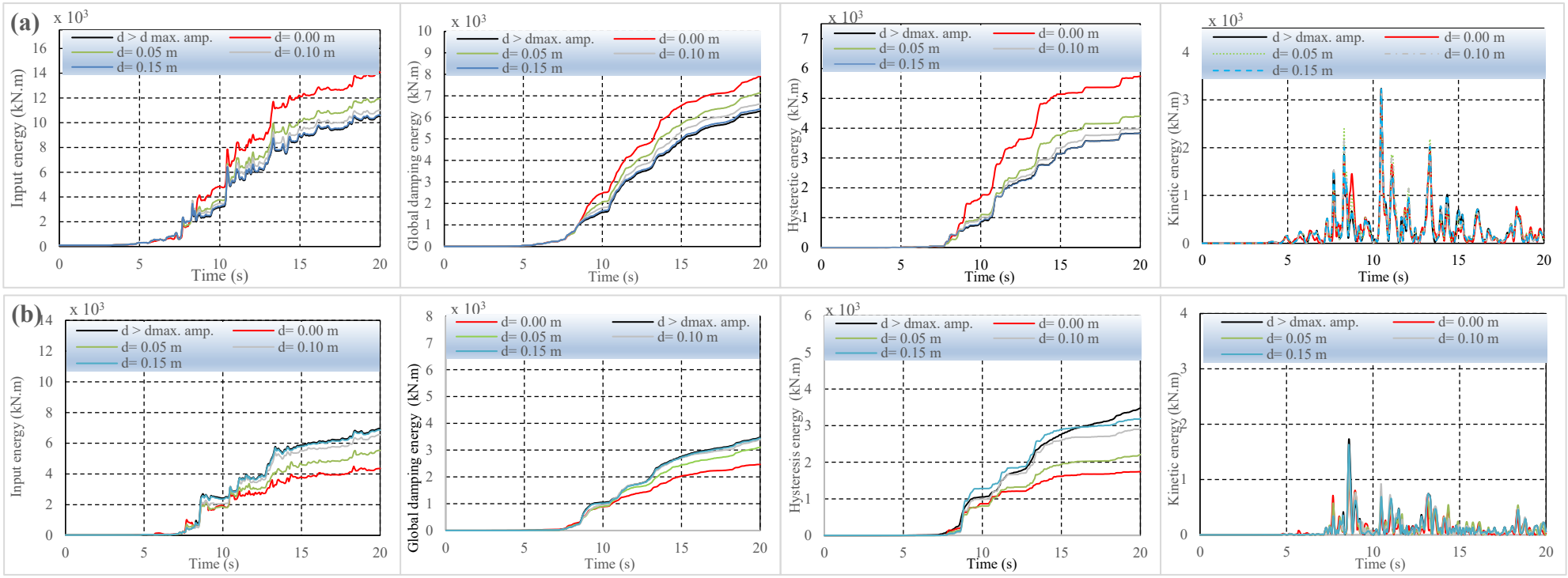

Fig.19 Input and dissipated energy time histories for adjacent buildings under Kobe (000)

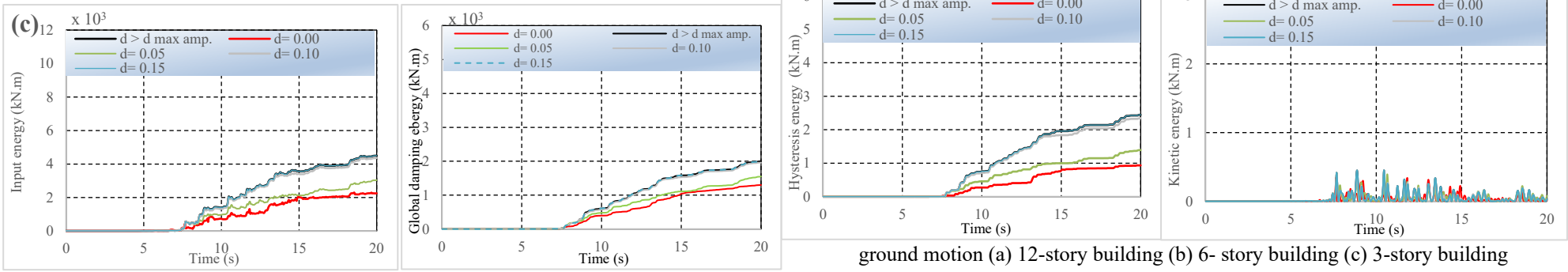

ground motion (a) 12-story building (b) 6- story building (c) 3-story building

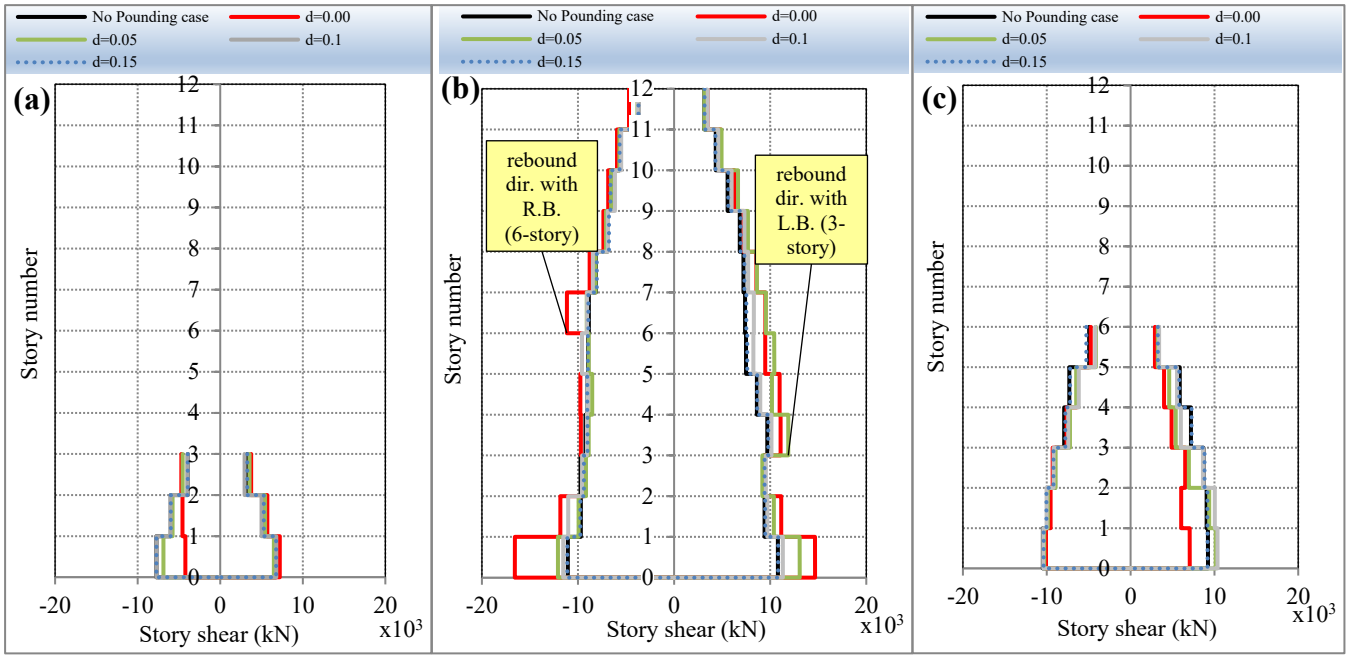

Fig. 20. Story shear forces responses under Kobe (000) earthquake records for different gap distance (a) 3-Story Building, (b) 12-Story-Building, (c) 6-Story Building

Figure 20 presents the induced story shear forces under Kobe (000) earthquake records for five gap sizes; d= 0.00 (full contact case), 0.05, 0.1, 0.15 in addition to no pounding case ($d > d_{max.\ Ampl}$). The figures reflect that the buildings models subjected to pounding force are extremely influenced by the gap distance between the collided building. The story shear forces of interior building (12-story) at base level are increased in case of full contact (d=0.00 m) by 50% at impact side with left building (3-Story) compared to no-pounding case while the magnification in corresponding impact side with right building (6-story) is 35%. Therefore, the pounding impacts are significantly influenced by the height ratio of the neighbouring structures. For the interior 12-story building, the impact between 12-story and 3-story experiences a greater response of story shear through the elevation above the top floor of the 3-story building in the rebound direction compared to the standalone collided buildings. Moreover, the 12-story and 6-story impact experiences a greater response of story shear through the elevation above the top floor of the 6-story building in the rebound direction compared to the standalone collided buildings. On contrary, the shear forces of exterior 3- and 6- story buildings are decreased in the direction of rebound relative to impact direction especially in contact case (d=0.00). Also, the variance in shear forces of the exterior buildings (3-story and 6-story) at the base level for different gap distances is slightly observed by shear envelopes in the impact side only relative to the rebound side due to one-sided impact. In contrast the interior building (12-story building), the variance in shear forces can be observed in the left and right sides due to two-sided impact. Pounding significantly affects the taller building's story shear in the stories above top level of the shorter building. At gap distance 0.15m, there is no influence of pounding and the curve almost matched with the fully separated case $d > d_{max.\ Ampl}$.

Figure 21 presents max story drifts responses under El Centro (180) earthquake record for d= 0.00 (full contact case), in addition to case of full separate, d > dmax. Ampl. The figures prove that the pounding can considerably change the response of story drifts. The drifts response of high-rise building (12- Story building) below the 3rd impact levels and above 6th impact level is increased at in-contact case (d =0.00 m) due to two-sided impact compared to full separated case. The drifts response of low-rise buildings (3-story and 6-story) are decreasing at in-contact case (d=0.00 m) compared to full separated case.

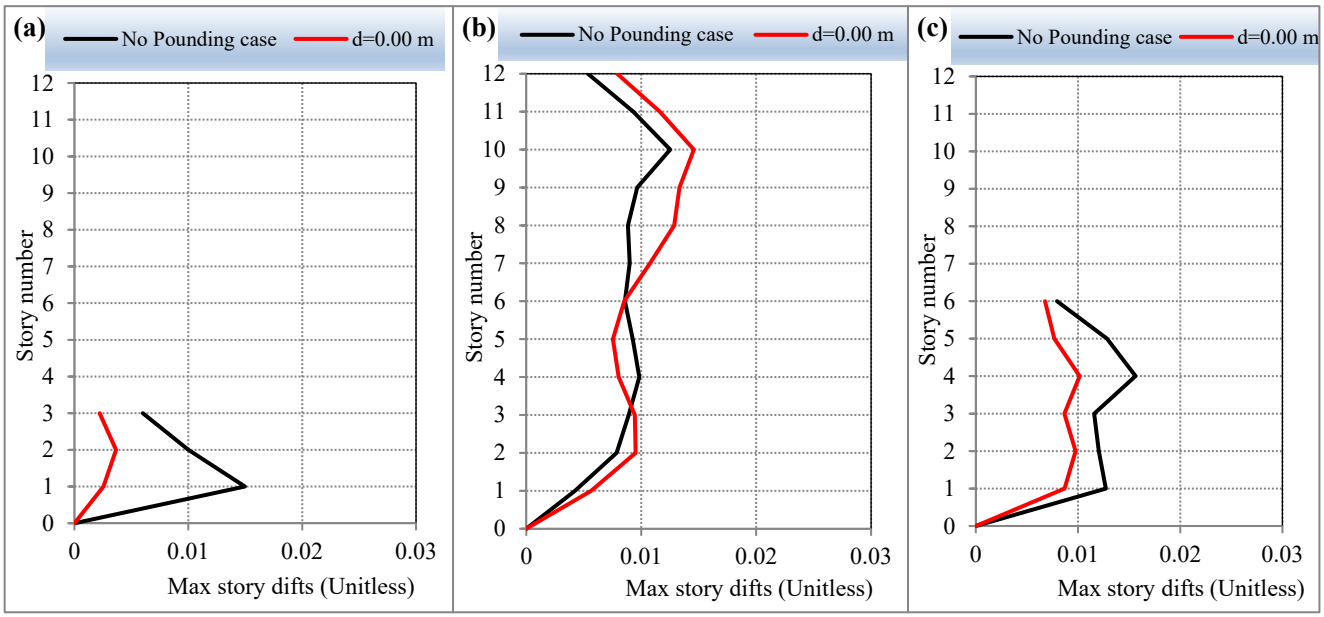

Fig. 21. Max story drifts responses under El Centro (180) earthquake record for different gap distance (a) 3-Story Building, (b) 12-Story-Building, (c) 6-Story Building

5.3 Changing in building performance level due to seismic pounding

The current study considering plastic hinges at every beam-column element at both ends which generate 960, 480 and 240 plastic hinges for 12 story, 6 story and 3 story buildings respectively. The following tables 7, 8, and 9 indicate the changing in local status of modelling parameters and acceptance criteria of plastic hinges for 12 story, 6 story and 3 story buildings respectively under Kobe (000) earthquake record. Pounding increases the maximum rotation of beam and column hinges, which causes an increase in the performance level of structural members and the structure itself. For the tall building (12-Story) the number of plastic hinges changed from linear status (A to IO) to non-linear status (IO to LS) are 74 and the number of hinges changed from (IO to LS) to (LS to CP) are 8. On the other hand, the modelling parameter has been changed from (B to C) or (A to B) to (>E) in 40 hinges which mean reaching to total collapse in those hinges. For smaller building (6-Story), the number of hinges changed from non-linear status to linear status are 30. While there are 14 hinges changed from total collapse status (>E) to (B to C) which indicate that the performance level of building has been decreased compared to the taller building.

Figure 22 presents influence of pounding on the global performance level of adjacent building in terms of immediate occupancy, life safety and collapse prevention D/C ratios. For the (12-story), the performance level of immediate occupancy (IO), live safety (LS) and Collapse prevention (CP) in contact case (d=0.00 m) has been increased by 33%, 142% and 140%, respectively as compared to the no pounding case. On the other hand, for the (6-story), the performance level of immediate occupancy (IO), live safety (LS) and Collapse prevention (CP) in contact case (d=0.00 m) has been decreased by 33%, 34%, and 34% (almost same) respectively as compared to the no pounding case. Similarly, for the (3-story), the performance level of immediate occupancy (IO), live safety (LS) and Collapse prevention (CP) in contact case (d=0.00 m) has been decreased by 18%, 17%, and 18% (almost same) respectively as compared to the no pounding case.

Table 10. introduce the change in acceptance criteria of the formed beam plastic hinges along height of 12-story building comparing the case of full-contact to non-pounding case under El Centro (180) earthquake record. The reduction of seismic performance level in beams, relative to no-pounding case, happens always in lower stories (from base level to 4 story level) under 3rd and 6th impact level. On the

contrary, an increase of performance level always is observed in the top stories (from 5 story level to 10 story level) along building height.

Table 7. Changing in modelling parameters and acceptance criteria of the formed plastic hinges for 12-story building comparing case of full-contact to no-pounding case under Kobe (000) earthquake record

Modelling parameter hinge state			Level changing description	Acceptance criteria hinge state			Level changing description
Non-pounding case	Pounding case d = 0.00 m	No. of P.H.		Non-pounding case	Pounding case d = 0.00 m	No. of P.H.	
A to B	B to C	64	increase	A to IO	IO to LS	74	increase
A to B	>E	8	increase	A to IO	LS to CP	6	increase
B to C	>E	32	increase	IO to LS	LS to CP	8	increase
B to C	A to B	4	decrease	LS to CP	>CP	8	increase
				IO to LS	A to IO	8	decrease
Total no. of changed P.H.		108				104	

Table 8. Changing in modelling parameters and acceptance criteria for 6-story building comparing case of full-contact to no-pounding case under Kobe (000) earthquake records

Modelling parameter hinge state			Acceptance criteria hinge state		
No pounding case	Pounding case d = 0.00 m	No. of P.H.	No pounding case	Pounding case d = 0.00 m	No. of P.H.
B to C	A to B	30	>CP	LS to CP	16
>E	B to C	14	IO to LS	A to IO	28
A to B	B to C	2	LS to CP	IO to LS	10
Total no. of changed P.H.		46			54

Table 9. Changing in modelling parameters and acceptance criteria for 3-story building comparing case of full-contact to no-pounding case under Kobe (000) earthquake records

Modelling parameter hinge state			Acceptance criteria hinge state		
No pounding case	Pounding case d = 0.00 m	No. of P.H.	No pounding case	Pounding case d = 0.00 m	No. of P.H.
A to B	B to C	18	A to IO	IO to LS	4
B to C	C to D	4	IO to LS	LS to CP	4
B to C	A to B	8	IO to LS	A to IO	8
C to D	B to C	6	LS to CP	IO to LS	6
Total no. of changed P.H.		36			22

Table: 10. Changing in acceptance criteria of the formed beam plastic hinges along height of 12-story building comparing case of full-contact to no-pounding case under El Centro (180) earthquake record

Story no.	Acceptance criteria hinge state			Level changing description
	No pounding case	Pounding case d = 0.00 m	No. of P.H.	
From story 10 to 5	A to IO	IO to LS	18	Increase
	IO to LS	LS to CP	2	Increase
From story 4 to 1	LS to CP	IO to LS	22	Decrease

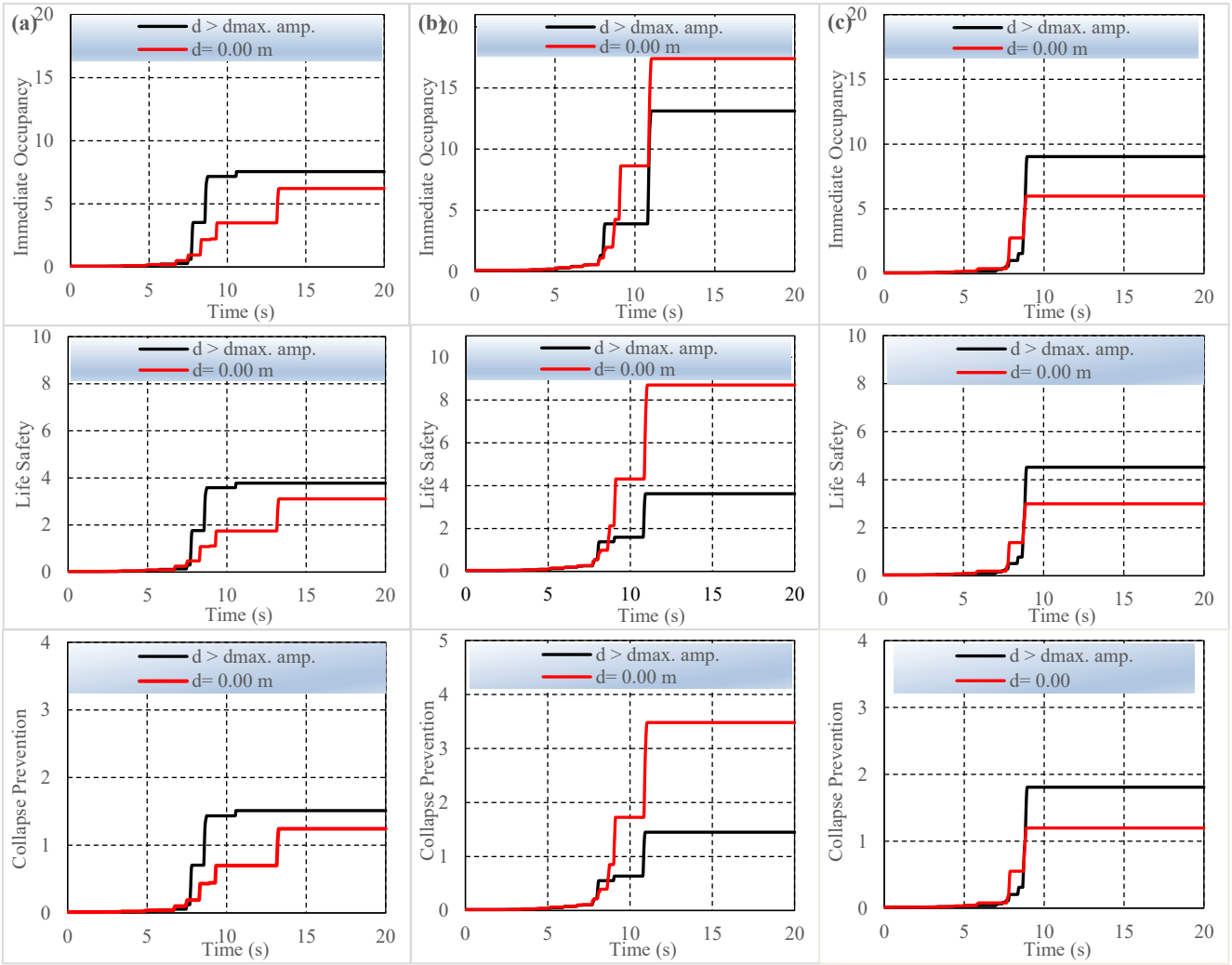

Fig.22. Influence of seismic pounding on the immediate occupancy, life safety and collapse prevention D/C ratios for the adjacent building under Kobe (000) earthquake (a) 3-Story building, (b) 12-Story building and (c) 6-story building.

6. Conclusions

The local and global seismic performance level of three different-height adjacent MRF buildings located side by side with pounding effect has been studied through nonlinear FE analysis by using ETABS V20.3.0 Build 2929. The main importance of the current study stems from the emphasis on an accurate modeling of the seismic pounding between adjacent buildings in series; geometrically as well as in terms of material nonlinearity, and a more reliable and quantitative investigation of the problem that would lead to more practical results. The pounding effect is investigated for different gap distances between adjacent buildings under strong ground motion and compared to the fully separate case. The global performance is assessed through the relative displacement, induced pounding force, story acceleration, story shear, story drifts, acceptance criteria in D/C ratio for buildings, and input and dissipated energy for buildings, while the local performance is assessed through hysteretic loops for selected elements such as the lower ground edge column and other formed plastic hinges at every beam-column connection. The numerical results obtained from this study confirm that the pounding interaction on the adjacent building's response is influenced by the following parameters:

- Dynamic properties of each building (fundamental period)

- Dynamic characteristics of ground motion
- Separation gap distance sizes
- The period ratio and height ratio of adjacent buildings
- The position of the building relative to other buildings; whether interior building with potential two-sided impact or an exterior building with potential one-sided impact.

Although the two ground motions have been scaled to 1.0g PGA to ensure the inelastic response of the structure, the response parameters are variant for each ground motion. It is observed that the high-rise building (12-story), irrespective of its pounding case, generates maximum story shear forces, story displacement, input energy, and dissipated energy. The seismic pounding limits the displacement on the impact side but can increase displacement responses on the rebound side (non-pounding side), especially true for the response of a 3-story building with a gap distance of 0.05 m under the El Centro (180) record and the case of in-contact under the Kobe (000) record. The acceleration response of the interior building (12-story building) beneath the levels of impact is substantially higher in each direction because of two-sided impact; the response gets its maximum values at the impact level and with a gap distance of 0.00 m and decreases effectively with the increase of gap size, while the response of the floors above the impact level is slightly affected. Moreover, the maximum responses of exterior buildings (6-story and 3-story buildings) are substantially higher in the directions of rebound throughout the building's height; however, the acceleration is marginally modified in the direction of impact because of a single-sided effect on the edge buildings of the alignment building configuration. The seismic pounding can significantly increase the response of input energy and the dissipated energy for the taller interior building (12-story building) relative to the case of non-pounding (buildings are fully separated), while the input energy and dissipated energy for the shorter exterior buildings (6- and 3-story buildings) are reduced relative to the case of non-pounding (buildings are fully separated). The building collision led to a change in the building's fundamental response to ground movements and transferred additional inertial loads and energy from the adjacent structure to the others. Collisions lead to a significant increase in the rotation value of the lower plastic hinge at the base column of the higher building as well as may result in a substantial increase in the range and intensity of damage at the base of the building. While the corresponding rotation values of the plastic hinge of the shorter building reduced significantly, therefore, the pounding severity is reduced.

In general, according to various response parameters that were mentioned previously, it has been concluded that the global performance of high-rise building (12-story) is significantly magnified, while the performance level of low-rise buildings (6-story and 3-story) is reduced. Although pounding may sometimes reduce the overall performance level of short buildings and thus be considered beneficial, more often it will amplify the response significantly of the relatively higher building, which may lead to total collapse. Therefore, it is highly recommended to introduce into the code’s conditions and provisions for the assessment of the minimum required seismic separation and the pounding risk of buildings.

7. Future Research Works

The three-buildings studies are symmetrical in plan and a single component of the ground motion is taken in the direction of pounding., However, an accidental torsion as requirement in Section 12.8.4.2 of ASCE 7-10 for buildings is considered.in the future studies, the pounding of asymmetric buildings under 3-components ground motions would be essential to investigated. The current study is theoretically explored using FE software. In future studies, it is crucial to experimentally study these characteristics using shaking table. Equal story height and floor to floor pounding is considered in the current study. The consideration of unequal story height and floor to column pounding need to be investigated in future studies. The stiffness and strength of the infilled wall has been ignored due to the difficulty to predict the masonry infill effect on the frame’s members, as different failure modes can

occur either in the masonry or in the surrounding frame. The contribution of stiffness and strength of infilled wall in addition to considering soft story effect is essential to be investigated in future studies.

References

1. Elwardany H, Mosa B, Khedr MDE, Seleemah A (2022) Effect of earthquake induced-pounding on the response of four adjacent buildings in series. Struct Eng Mech 83:153–166. https://doi.org/10.12989/sem.2022.83.2.153
2. Efraimiadou S, Hatzigeorgiou GD, Beskos DE (2013) Structural pounding between adjacent buildings subjected to strong ground motions. Part I: the effect of different structures arrangement. Earthq Eng Struct Dyn 42:1509–1528. https://doi.org/10.1002/eqe.2285
3. Rojas FR, Anderson JC (2012) Pounding of an 18-story building during recorded earthquakes. J Struct Eng 138:1530–1544. https://doi.org/10.1061/ (ASCE) ST. 1943- 541X. 00005 41
4. Sołtysik B, Jankowski R (2015) Building damage due to structural pounding during earthquakes. J Phys: Conf Ser 628:012040
5. Crozet V, Politopoulos I, Yang M et al (2017) Influential structural parameters of pounding between buildings during earthquakes. Procedia Eng 199:1092–1097. https://doi.org/10.1016/j.proeng.2017.09. 084
6. Crozet V, Politopoulos I, Yang M et al (2018) Sensitivity analysis of pounding between adjacent structures. Earthq Eng Struct Dyn 47:219–235. https://doi.org/10.1002/eqe.2949
7. Elwardany H, Seleemah A, Jankowski R (2017) Seismic pounding behavior of multi-story buildings in series considering the effect of infill panels. Eng Struct 144:139–150. https://doi.org/10.1016/j.engstruct.2017.01.078
8. Elwardany H, Seleemah A, Jankowski R (2018) Corrigendum to "Seismic pounding behavior of multi-story buildings in series onsidering the effect of infill panels" [Eng Struct 144 (2017) 139–150]. Eng Struct 171–933
9. Ismail R, Hasnan MH, Shamsudin N (2017) Structural pounding of concrete frame structure with masonry infill wall under seismic loading. In: AIP conference proceedings. AIP Publishing LLC, p 120011
10. Manoukas GE, Karayannis CG (2024) Asymmetric seismic pounding between multistorey reinforced concrete structures in a city block. Soil Dyn Earthq Eng 177:108415. https://doi.org/ 10.1016/j. soil dyn. 2023. 108415
11. Mavronicola EA, Polycarpou PC, Komodromos P (2017) Spatial seismic modeling of base-isolated buildings pounding against moat walls: effects of ground motion directionality and mass eccentricity. Earthq Eng Struct Dyn 46:1161–1179. https://doi.org/10.1002/eqe.2850
12. Mavronicola EA, Polycarpou PC, Komodromos P (2020) Effect of ground motion directionality on the seismic response of base isolated buildings pounding against adjacent structures. Eng Struct 207:110202. https://doi.org/10.1016/j.engstruct.2020.110202
13. Mahmoud S, Jankowski R (2010) Pounding-involved response of isolated and non-isolated buildings under earthquake excitation.Earthq Struct 1:231–252
14. Pant DR, Wijeyewickrema AC (2012) Structural performance of a base-isolated reinforced concrete building subjected to seismic pounding. Earthq Eng Struct Dyn 41:1709–1716. https://doi.org/10.1002/ eqe.2158
15. Liu C, Yang W, Yan Z et al (2017) Base pounding model and response analysis of base-isolated structures under earthquake excitation. Appl Sci 7:1238
16. Far H (2019) Advanced computation methods for soil-structure interaction analysis of structures resting on soft soils. Int J Geotech Eng 13:352–359. https://doi.org/10.1080/19386362.2017.1354510
17. Chinmayi HK (2019) Study on pounding of structures with soil–structure interaction effects: a review. J Instit Eng Ser A100:199–204. https://doi.org/10.1007/s40030-018-0341-4
18. Sobhi P, Far H (2021) Impact of structural pounding on structural behaviour of adjacent buildings considering dynamic soil-structure interaction. Bull Earthq Eng 20:3515–3547. https://doi.org/10.1007/s10518-021-01195-w
19. Fatahi B, Van Nguyen Q, Xu R, Sun W (2018) Three-dimensional response of neighboring buildings sitting on pile foundations to seismic pounding. Int J Geomech 18:04018007

20. Miari M, Jankowski R (2022) Shaking table experimental study on pounding between adjacent structures founded on different soil types. Structures 44:851–879. https://doi.org/10.1016/j.istruc.2022.08.059
21. American Society of Civil Engineers (ASCE) (2016) Minimum design loads for buildings and other structures: ASCE/SEI 7–16.
22. Naseri SA, VaseghiAmiri J, Rajabnejad H, Sadeghi A (2022) A study into the effect of different ground motion durations on the seismic pounding force by considering soil–structure interaction. Asian J Civ Eng 23:53–65. https://doi.org/10.1007/s42107-021-00408-6
23. Computers and Structures Inc. (CSI) (2022) ETABS2022 Ultimate C v20.3.0 Build 2929. Computers and Structures Inc., Berkeley.
24. FEMA-356. Prestandard and commentary for the seismic rehabilitation of buildings. Federal Emergency Management Agency. Washington DC: 2000.
25. ASCE41-17. Seismic Evaluation and Retrofit of Existing Buildings In: ASCE/SEI standard 41-17. American Society of Civil Engineers. Reston: 2017. 10.1061/9780784414859.
26. A.K. Chopra, Dynamics of structures, 3rd edition, Prentice Hall, NJ, 2006.
27. Mander JB, Priestley MJN, Park R (1988) Theoretical stress–strain model for confined concrete. J Struct Eng 114(8):1804–1826.
28. Watanabe G, Kawashima K (2004) Numerical simulation of pounding of bridge decks. In: The 13th world conference on earthquake engineering, Vancouver, BC, Canada.
29. Maison BF, Kasai K (1992) Dynamics of pounding when two buildings collide. Earthq Eng Struct Dyn 21:771–786.
30. Anagnostopoulos SA (1988) Pounding of buildings in series during earthquakes. Earthq Eng Struct Dyn 16:443–456.
31. Kawashima K, Shoji G (2000) Effect of restrainers to mitigate pounding between adjacent decks subjected to a strong ground motion. In: 12th world conference on earthquake engineering, New Zealand, Auckland, Paper no. 1435.
32. Guo A, Cui T, Li H (2012) Impact stiffness of the contact-element models for the pounding analysis of highway bridges: experimental evaluation. J Earthq Eng 16(8):1132–1160.
33. Jankowski R (2006) Pounding force response spectrum under earthquake excitation. Eng Struct 28:1149–1161.
34. Shakya K, Wijeywickrema AC, Ohmachi T (2008) Mid-column seismic pounding of reinforced concrete buildings in a row considering effects of soil. In: 14th WCEE, Beijing, Paper ID 05-01-0056.
35. Pacific Earthquake Engineering Research Center (PEER) (2013). PEER NGA-West2 database. PEER report 2013/03, Pacific Earthquake Engineering Research Center, University of California, Berkeley.
36. Housing and Building National Research Center (ECP) (1993) ECP-201: Egyptian code for calculating loads and forces in structural work and masonry. Ministry of Housing, Utilities and Urban Planning
37. Housing and Building National Research Center (ECP) (2008) ECP-201: Egyptian code for calculating loads and forces in structural work and masonry. Ministry of Housing, Utilities and Urban Planning
38. National Research Council of Canada (NRCC) (2005) NBCC: national building code of Canada, 12th edn. Canadian Commission on Building and Fire Codes, National Research Council of Canada, Ottawa.
39. European Committee for Standardization (CEN) (2004) Eurocode 8: design of structures for earthquake resistance—part 1: general rules, seismic actions and rules for buildings (EN 1998–1). Belgium